




















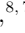



## UNCOVER: 404 Error – Models Not Found for the Triply Imaged Little Red Dot A2744-QSO1

YILUN MA (马逸伦) <sup>1</sup>, JENNY E. GREENE <sup>1</sup>, DAVID J. SETTON <sup>1</sup>, MARTA VOLONTERI <sup>2</sup>, JOEL LEJA <sup>3,4,5</sup>,  
BINGJIE WANG (王冰洁) <sup>3,4,5</sup>, RACHEL BEZANSON <sup>6</sup>, GABRIEL BRAMMER <sup>7</sup>, SAM E. CUTLER <sup>8</sup>, PRATIKA DAYAL <sup>9</sup>,  
PIETER VAN DOKKUM <sup>10</sup>, LUKAS J. FURTAK <sup>11</sup>, KARL GLAZEBOOK <sup>12</sup>, ANDY D. GOULDING <sup>1</sup>,  
ANNA DE GRAAFF <sup>13</sup>, VASILY KOKOREV <sup>14</sup>, IVO LABBÉ <sup>15</sup>, RICHARD PAN <sup>16</sup>, SEDONA H. PRICE <sup>6</sup>,  
JOHN R. WEAVER <sup>8</sup>, CHRISTINA C. WILLIAMS <sup>17</sup>, KATHERINE E. WHITAKER <sup>8,7</sup> AND ADI ZITRIN <sup>18</sup>

<sup>1</sup>*Department of Astrophysical Sciences, Princeton University, Princeton, NJ 08544, USA*

<sup>2</sup>*Institut d’Astrophysique de Paris, Sorbonne Université, CNRS, UMR 7095, 98 bis bd Arago, F-75014 Paris, France*

<sup>3</sup>*Department of Astronomy & Astrophysics, The Pennsylvania State University, University Park, PA 16802, USA*

<sup>4</sup>*Institute for Computational & Data Sciences, The Pennsylvania State University, University Park, PA 16802, USA*

<sup>5</sup>*Institute for Gravitation and the Cosmos, The Pennsylvania State University, University Park, PA 16802, USA*

<sup>6</sup>*Department of Physics and Astronomy and PITT PACC, University of Pittsburgh, Pittsburgh, PA 15260, USA*

<sup>7</sup>*Cosmic Dawn Center (DAWN), Niels Bohr Institute, University of Copenhagen, Jagtvej 128, København N, DK-2200, Denmark*

<sup>8</sup>*Department of Astronomy, University of Massachusetts, Amherst, MA 01003, USA*

<sup>9</sup>*Kapteyn Astronomical Institute, University of Groningen, P.O. Box 800, 9700 AV Groningen, The Netherlands*

<sup>10</sup>*Department of Astronomy, Yale University, New Haven, CT 06511, USA*

<sup>11</sup>*Physics Department, Ben-Gurion University of the Negev, P.O. Box 653, Be’er-Sheva 84105, Israel*

<sup>12</sup>*Centre for Astrophysics and Supercomputing, Swinburne University of Technology, PO Box 218, Hawthorn, VIC 3122, Australia*

<sup>13</sup>*Max-Planck-Institut für Astronomie, Königstuhl 17, D-69117, Heidelberg, Germany*

<sup>14</sup>*Department of Astronomy, The University of Texas at Austin, Austin, TX 78712, USA*

<sup>15</sup>*Centre for Astrophysics and Supercomputing, Swinburne University of Technology, Melbourne, VIC 3122, Australia*

<sup>16</sup>*Department of Physics and Astronomy, Tufts University, 574 Boston Ave, Medford, MA 02155, USA*

<sup>17</sup>*NSF National Optical-Infrared Astronomy Research Laboratory, 950 North Cherry Avenue, Tucson, AZ 85719, USA*

<sup>18</sup>*Department of Physics, Ben-Gurion University of the Negev, P.O. Box 653, Be’er-Sheva 84105, Israel*

(Received MMDDYY; Revised MMDDYY; Accepted MMDDYY)

Submitted to ApJ

### ABSTRACT

*JWST* has revealed an abundance of compact, red objects at  $z \approx 5 - 8$  dubbed “little red dots” (LRDs), whose SEDs display a faint blue UV continuum followed by a steep rise in the optical. Despite extensive study of their characteristic V-shaped SEDs, the nature of LRDs remains unknown. We present a new analysis of the NIRSpect/PRISM spectrum of A2744-QSO1, a triply imaged LRD at  $z = 7.04$  from the UNCOVER survey. The spectrum shows a strong Balmer break and broad Balmer emission lines, both of which are difficult to explain with models invoking exclusively AGN or stellar contributions. Our fiducial model decomposes the spectrum into a post-starburst galaxy dominating the UV-optical continuum and a reddened AGN being sub-dominant at all wavelength and contributing at  $\sim 20\%$  level. However, our most credible model infers a stellar mass of  $M_\star \approx 4 \times 10^9 M_\odot$  within a radius of  $r_e < 30$  pc, driving its central density to the highest among observations to date. This high central density could be explained if A2744-QSO-1 is the early-forming core of a modern-day massive elliptical galaxy that later puffed up via the inside-out growth channel. The models also necessitate an unusually steep dust law to preserve the strong break strength, though this steepness may be explained by a deficit of large dust grains. It is also probable that these challenges reflect our ignorance of A2744-QSO1’s true nature. Future variability and reverberation mapping studies could help disentangle the

galaxy and AGN contribution to the continuum, and deeper redder observations could also unveil the dust properties in LRDs.

*Keywords:* Active galactic nuclei (16), Black holes (162), Galaxy formation (595), High-redshift galaxies (734)

## 1. INTRODUCTION

Before the launch of *James Webb Space Telescope* (*JWST*; Gardner et al. 2023), galaxies and active galactic nuclei (AGN) were often discovered by rest-frame ultraviolet (UV) selection methods and/or drop-out techniques at  $z \gtrsim 4$  (e.g., Fan et al. 2001; Bouwens et al. 2015). However, these UV-selection methods tend to be biased towards preferentially selecting the most massive and luminous black holes (BHs) in the early universe (Fan et al. 2023). Thanks to its high sensitivity and spatial resolution, *JWST* has revolutionized our understanding of black holes in the high-redshift universe by enabling detections of fainter sources, instead of solely the brightest AGN and quasars (Goulding et al. 2023; Harikane et al. 2023; Maiolino et al. 2023).

One of the most intriguing results from *JWST* is the discovery of a population of compact red sources at high redshift (Furtak et al. 2023a; Labbe et al. 2023; Akins et al. 2024; Barro et al. 2024; Kocevski et al. 2024; Kokorev et al. 2024a). Because of their size and colour, these sources are dubbed little red dots (LRDs; Matthee et al. 2024). The LRDs are identified from photometric samples for their V-shaped photometric spectral energy distribution (SED), which consists of a faint blue ultraviolet (UV) continuum followed by a steep red rise in continuum flux into the rest-frame optical wavelengths.

Motivated by the compact sizes ( $r_e \approx 100$  pc; Labbe et al. 2023; Akins et al. 2024) of these objects, photometric SED modeling analyses have often invoked an AGN component on top of a galaxy SED (e.g., Furtak et al. 2023a; Barro et al. 2024; Pérez-González et al. 2024). Indeed, in follow-up spectroscopic programs, nearly 80% of the photometrically selected LRDs show broad Balmer and Paschen emission lines with FWHM  $> 2000$  km s $^{-1}$  typically seen in type-1 AGNs (e.g., Kocevski et al. 2023; Greene et al. 2024; Furtak et al. 2024; Matthee et al. 2024; Wang et al. 2024a). The common presence of broad lines corroborates the potential existence of massive BHs in LRDs. If one takes the BH mass estimates inferred from emission line scaling relations at face value, LRDs would host overmassive BHs when compared to their host galaxies ( $M_{\text{BH}}/M_{\star} \approx 1\%$ ; Kokorev et al. 2023; Furtak et al. 2024; Wang et al. 2024b). These BH mass measurements also imply that the BHs in LRDs accrete at high Eddington ratios (Furtak et al. 2024; Greene

et al. 2024). Many other BH seeding and growth mechanisms such as primordial origins (Dayal 2024) and prolonged accretion in high-density environments (Inayoshi & Ichikawa 2024) have also been proposed for these intriguing objects.

Another important point is that LRDs have a surprisingly high number density of roughly  $10^{-5}$  Mpc $^{-3}$  mag $^{-1}$  for  $z > 4$  (Greene et al. 2024; Matthee et al. 2024; Kocevski et al. 2024). Both Akins et al. (2024) and Greene et al. (2024) find that LRDs are  $\sim 100$  times more common than one would expect if simply extrapolating the UV luminosity functions of high-redshift quasars to match the UV luminosity of LRDs; they also account for 1% of the UV-selected galaxies at  $z \approx 4 - 6$ . Moreover, Kocevski et al. (2024) find that the number density of LRDs photometrically selected by rest-frame spectral slopes drop significantly at  $z \lesssim 4$ . This could suggest that LRDs may mark a previously unknown and poorly understood episode of BH growth prevalent in the early universe.

Nevertheless, despite extensive theoretical and observational studies on these intriguing sources, the nature of LRDs is still uncertain. Many models can fit parts of their SEDs well, but no comprehensive model describing all of their observed features has yet taken hold. The UV can be described by both unobscured scattered light from the central BH and/or a dust-free stellar population, whereas the red optical can be described by either a reddened AGN or an attenuated stellar component (Killi et al. 2023; Greene et al. 2024; Pérez-González et al. 2024; Wang et al. 2024a; Williams et al. 2024). Beyond the UV-optical regime, the flattening of rest-frame near-infrared (Williams et al. 2024), X-ray non-detections (Akins et al. 2024; Yue et al. 2024), and the lack of a rising continuum associated with the host dust typically observed in dust-reddened AGN in the mid-infrared wavelengths of LRDs (Akins et al. 2024; Wang et al. 2024a) are often interpreted as significant challenges to the AGN interpretation, leading to the stellar origin of LRDs. However, such explanations cannot easily reconcile with the uncomfortably efficient early formation history (Wang et al. 2024b) and the existence of broad lines (Maiolino et al. 2024a), although the feasibility of such scenario has been suggested by Baggen et al. (2024). The X-ray non-detections have also been

interpreted as evidence for super-Eddington AGN (e.g., Lambrides et al. 2024; Pacucci & Narayan 2024), but the exact SED shape for such accretors is highly uncertain and poorly understood (e.g., Kubota & Done 2019).

The challenges in understanding the SED of LRDs are only complicated further by their faintness ( $-20 \lesssim M_{UV} \lesssim -16$ ). Fortunately, foreground galaxy clusters can serve as gravitational lenses to efficiently obtain high-SNR spectra of LRDs and conduct detailed modeling of their SED shapes. In this work, we present a spectral analysis that decomposes the UV-optical continuum emission of A2744-QSO1, a triply imaged LRD at  $z = 7.04$  in the Ultradeep NIRSpec and NIRCам Observations before the Epoch of Reionization (UNCOVER) survey that displays a strong break feature at rest-frame  $\sim 3600 \text{ \AA}$  in its rest-frame UV-optical spectrum (Furtak et al. 2023a, 2024). Section 2 describes the observations, the data, and our knowledge of the properties of A2744-QSO1 to date. In Section 3, we present our spectral analysis with multiple models to decompose A2744-QSO1’s continuum emission. Lastly, we discuss some of the challenges in the modeling process in Section 4. Throughout this work, we assume a cosmology of  $\Omega_{m,0} = 0.3$ ,  $\Omega_{\Lambda,0} = 0.7$ , and  $H_0 = 70 \text{ km s}^{-1} \text{ Mpc}^{-1}$ . All magnitudes are expressed in AB magnitudes.

## 2. DATA AND SOURCE DESCRIPTION

### 2.1. Observations

The UNCOVER survey (Bezanson et al. 2022) is a *JWST* Cycle 1 Treasury program. It was designed to exploit the foreground galaxy cluster Abell 2744 ( $z = 0.308$ ; Lotz et al. 2017) as a gravitational lens to obtain deep NIRCам broad-band imaging, photometrically detecting sources with  $m_{F444W} \lesssim 30 \text{ mag}$  for characterization (Weaver et al. 2024). In addition, medium-band imaging from observations taken in Cycle 2 are also available for most of the  $45 \text{ arcmin}^2$ -field as part of the Medium Bands, Mega Science survey (Suess et al. 2024).

A2744-QSO1 was observed as part of the NIRSpec/PRISM follow-up campaign of the UNCOVER survey, which includes 668 unique targets (Price et al. 2024). The spectroscopic observations used a 2-POINT-WITH-NIRCам-SIZE2 dither pattern and nodded with a 3 shutter slitlet pattern with the apertures at a position angle of  $44.56$  degrees. The three images of A2744-QSO1 were included in five (A), three (B), and four (C) of the seven micro-shutter array (MSA) mask configurations, respectively. The total exposure times for the three images are 16.7 hours (A), 9.4 hours (B), and 11.7 hours (C), respectively.

### 2.2. Data Reduction

Price et al. (2024) provide the full detailed description of the reduction process of the NIRSpec/PRISM spectrum, so we only give a brief summary here. We begin with level 1 products from MAST<sup>1</sup> and run the *JWST* `jwst` (Bushouse et al. 2024) stage 1 pipeline with `msaexp` (Brammer 2023a) and `grizli` (Brammer 2023b); snowballs are corrected in this process. We then correct for the  $1/f$  noise and the bias offset. World coordinate system (WCS) assignments, 2D slits extraction, slit flat-fielding, vignetting correction, and photometric calibration are carried out in the `jwst` stage 2 pipeline. We subtract the local background by taking the difference of frames at different nodding positions. The background-subtracted exposures are then drizzle resampled onto a common grid before aligning and stacking. Finally, we modify the optimal extraction algorithm by Horne (1986) to account for the wavelength-dependent PRISM resolution and extract the final 1D spectrum. We do not combine the spectra of all three images and only utilize the one to image A (MSA 13123) in UNCOVER/Mega Science Data Release 4 (DR4) for the analysis. This is to avoid possible spectral shape changes among the different gravitationally lensed images due to potential time variability (Golubchik et al. 2024; Kokubo & Harikane 2024). The final 1D-spectrum is offset from the photometry by a roughly constant factor of  $\sim 1.1$ , which is likely due to imperfect slit loss corrections, but the continuum shape is not affected.

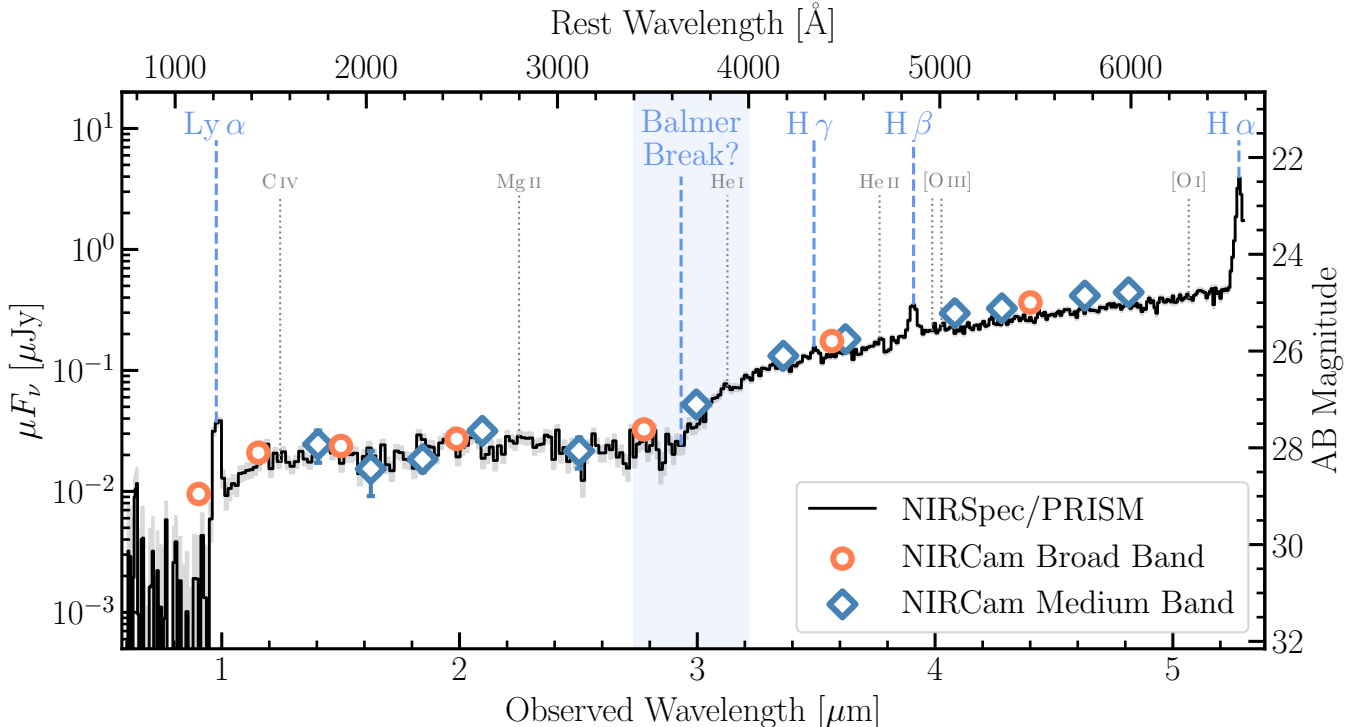
In this work, we adopt a lensing magnification of  $\mu = 5.4 \pm 0.1$ , corresponding to the image covered by MSA13123 (image A; Furtak et al. 2024) to de-magnify the spectrum in our modeling procedures. Taken the magnification into account, the effective exposure time on our spectrum is approximately 90 hours. The tangential magnification, used for size constraints, is  $\mu_t = 3.21 \pm 0.05$ . The magnifications are computed at the position of image A and the redshift of the source from the latest UNCOVER strong-lensing model of Abell 2744. The parametric lens model of the cluster was initially constructed in Furtak et al. (2023b) using the Zitrin et al. (2015) analytic method and `v2.0` has been updated with *JWST* spectroscopic redshifts in Price et al. (2024). The model is publicly available in DR4 on the UNCOVER website<sup>2</sup>.

### 2.3. A2744-QSO1

A2744-QSO1 is the first LRD discovered in the UNCOVER field, selected for its compact size and V-shaped photometric SED shape (Furtak et al. 2023a). It is also

<sup>1</sup> Available from: <https://dx.doi.org/10.17909/8k5c-xr27>

<sup>2</sup> <https://jwst-uncover.github.io/DR4.html>



**Figure 1.** The NIRSpect/PRISM spectrum of image A (MSA13123) of A2744-QSO1 with no lensing correction applied is shown in black. The shaded gray area around the flux is the  $1\sigma$ -range of the observed spectrum. The circles and diamonds are photometry from the NIRCam broad-band and medium-band filters, respectively (Suess et al. 2024). Strong hydrogen emission lines and the break are labelled in blue. Helium and metal lines are labelled in gray.

the LRD with the best size constraint due to its image multiplicity and the strong lensing magnification in the UNCOVER field. The three images of the object are all consistent with point sources across all the NIRCam filters. An upper limit of  $r_e < 30$  pc is thus estimated based on the lensing magnification and the point spread function in the F115W band (Furtak et al. 2023a, 2024). Given some LRDs show signatures of extended morphology in the UV (e.g., Kokorev et al. 2024b; Labbé et al. in prep.), it is likely that this size upper limit probes the physical extent of the stellar populations in A2744-QSO1. Yet, we also note that spatially extended scattered light has been observed in low-redshift AGN as well (e.g., Zakamska et al. 2005, 2006). Indeed, in order to model the photometric SED of A2744-QSO1 and to explain its compactness, Furtak et al. (2023a) prefer a model where the UV continuum originates from the unobscured scattered AGN light and the optical continuum is produced by a reddened AGN.

The low-resolution NIRSpect/PRISM spectrum of A2744-QSO1, shown in Figure 1, confirms the source redshift at  $z_{\text{spec}} = 7.04$  (Furtak et al. 2024). The spectrum reveals broad Balmer emission lines with  $\text{FWHM} \approx 2500 \text{ km s}^{-1}$  (Furtak et al. 2024) — such line widths are typically seen in type-1 AGNs, corroborating

the potential existence of a BH. The authors also measure line luminosities of  $L_{\text{H}\alpha} = 7.1 \pm 0.3 \times 10^{41} \text{ erg s}^{-1}$  and  $L_{\text{H}\beta} = 9.5 \pm 0.3 \times 10^{40} \text{ erg s}^{-1}$ ; in contrast, the metal lines are very weak. Based on the line width and luminosity, Furtak et al. (2024) estimate that A2744-QSO1 hosts a BH with  $M_{\text{BH}} = 4_{-1}^{+2} \times 10^7 M_{\odot}$  that is accreting at 30% of its Eddington luminosity, although one should be cautious about inferring  $M_{\text{BH}}$  using standard scaling relations at such high redshift (King 2024; Lupi et al. 2024). Equally prominent in the PRISM spectrum in Figure 1 is a discontinuity and change in continuum slope at  $\sim 3 \mu\text{m}$  observed frame (referred as “the break” hereafter). It is worth noting that the break coincides with 3600–4000 Å in the rest-frame where continuous Balmer absorption occurs, hinting at a continuum signature of the galaxy host. Assuming the highest surface density observed to date (Baggen et al. 2023; Vanzella et al. 2023), Furtak et al. (2024) estimates a fiducial stellar mass upper limit of  $M_{\star} < 1.4 \times 10^9 M_{\odot}$ . Nevertheless, the authors do not conduct a detailed analysis of the continuum to support their inferred stellar mass upper limit.

### 3. MODELING



Given all of the information mentioned above, we aim to search for a self-consistent model capable of explaining all of the observables. In this section, we present several SED fits that we perform on the de-magnified spectrum of A2744-QSO1. The SED models are produced using combinations of AGN continua and synthesized high-resolution spectra of composite stellar populations. We first make a few general comments applicable to all the modeling procedures in this work before delving into the different options to model the spectrum of A2744-QSO1.

### 3.1. Overall Settings

Throughout our analysis, we conduct the spectral fitting with `PyMultiNest` (Buchner et al. 2014; Feroz & Hobson 2008; Feroz et al. 2009, 2019), a nested sampling code. Such an algorithm is particularly useful when multiple modes potentially exist in the posterior distributions.

We model the continuum emission of A2744-QSO1 without emission lines. The strong emission lines have significant broad components and may also harbor narrow components, both of which can vary in width and fractional contribution from one line to another — this is difficult to disentangle at the low resolution of the PRISM spectra and is outside of the scope of this work. Additionally, Furtak et al. (2024) and Greene et al. (2024) already provide an extensive analysis and discussion of the emission lines of A2744-QSO1 and of the LRDs in the UNCOVER field. Since the metal emission lines are very weak for A2744-QSO1, as shown in Figure 1, modeling the continuum alone is much easier than in the case of some other LRDs (Labbé et al. in prep.). Therefore, we mask at the positions of strong broad emission lines, i.e.,  $H\alpha$ ,  $H\beta$ , and  $H\gamma$ , to avoid complications in the modeling process. We also mask  $\lambda_{\text{rest}} < 1400 \text{ \AA}$  since the physical origin of this UV emission remains ambiguous. The flux drop just redward of the  $\text{Ly}\alpha$  emission line may be due to the damped wing of  $\text{Ly}\alpha$  absorption in the circumgalactic medium. It could also be attributed to the two-photon continuum (Cameron et al. 2024; Katz et al. 2024), although we do not detect the recombination edge of the hydrogen nebular continuum that is usually associated with it.

Next, we proceed to calibrate the spectral resolution. The model spectra output from stellar population synthesis codes are of much higher resolution than those observed by the NIRSpec/PRISM. The published resolution curve by Jakobsen et al. (2022) and that on the *JWST* user documentation webpage are calibrated using uniformly illuminated slits. de Graaff et al. (2024a) show that point sources would yield up to a factor of  $\sim 2$

higher spectral resolution. Since A2744-QSO1 is unresolved throughout all the NIRCcam bands as we mention in Section 2, this is the appropriate regime in our case. After accounting for the additional broadening in the reduction and coadding processes, we conservatively increase the published spectral resolution by a factor of 1.3 at all wavelengths for simplicity and convolve the model spectra to this resolution before comparing it to the observed data, similar to the treatment by Greene et al. (2024). Using the more realistic wavelength- and size-dependent correction factor mostly affects the line width measurements rather than continuum modeling. We also test other constant factors ranging from 1 to 1.8 and confirm that the continuum shape, including the break, is not sensitive to the specific value of this correction factor. The model and observed spectra are compared in  $\log F_\nu$  versus wavelength (as shown in Figure 1 and Figure 2).

Lastly, we note that similar spectral decomposition analysis of LRDs has been carried out in the literature (e.g., Wang et al. 2024a,b). Our modeling procedures are similar to those works in many respects (see descriptions in the following sections), but there is one specific difference that we highlight here. The authors conduct additional steps such as polynomial calibration of spectroscopic continuum to photometry and error inflation in the modeling processes to account for slit losses and other data quality/calibration issues. These steps may also leave room to potentially mitigate shortcomings in the models themselves. However, since the spectrum of image A of A2744-QSO1 has a very high SNR  $\approx 20$  per pixel, and the medium band photometry of A2744-QSO1 confirms the spectral shape (Furtak et al. 2024, and Figure 1), we omit these additional steps and take the data as it is for our modeling analysis hereafter.

### 3.2. AGN-Only Model

The broad Balmer emission lines displayed in the spectrum of A2744-QSO1 as well as its compact morphology are the major arguments for the presence of an AGN (Furtak et al. 2024; Greene et al. 2024). Somewhat similar populations of reddened broad-line AGN are known at lower redshift (e.g., Glikman et al. 2012; Banerji et al. 2015). Therefore, we use the preferred AGN-only model from Furtak et al. (2023a) as a starting point and test its validity in explaining the spectral shape. In brief, this model attributes the optical flux to a reddened AGN

**Table 1.** Free Parameters and Their Priors in the modeling

Parameter	Unit	Description	Prior
$\log M_*$	$M_\odot$	Total stellar Mass	[7, 12]
$\log \tau$	Gyr	$e$ -folding timescale in a delayed- $\tau$ star formation history	[-3.3, 1]
$t_{\text{start}}$	Gyr	Starting time of the delayed- $\tau$ star formation history	[0, $t_{\text{universe}}$ ]
$A_V^{\text{gal}}$	mag	$V$ -band attenuation of the stars (also seen by the AGN)	[0, 5]
$\delta$	—	Multiplicative power law index of the <a href="#">Noll et al. (2009)</a> dust law	[-1, 0.4]
$f_{\text{nodust}}$	—	Fraction of stars not experiencing any dust attenuation	[0, 1]
$\log \lambda L_{\lambda,3000}$	$\text{erg s}^{-1}$	Luminosity of the unreddened AGN continuum at rest-frame 3000 Å	[43, 47]
$A_V^{\text{AGN}}$	mag	$V$ -band extinction of the AGN (not seen by the stars)	[0, 5]
$f_{\text{scat}}$	—	Fraction of light scattered from the unreddened AGN continuum	[0, 1]
$\log M_{\text{BH}}$	$M_\odot$	Black hole mass	[6, 9]

NOTE—The table presents all free parameters invoked in this work. A given model does not necessarily involve all the free parameters listed above. All priors are uniform within the ranges. The age of the universe  $t_{\text{universe}}$  at  $z = 7.04$  is 0.745 Gyr under the concordance cosmology assumed in this work.

**Table 2.** Best-Fit Parameters in Different Models

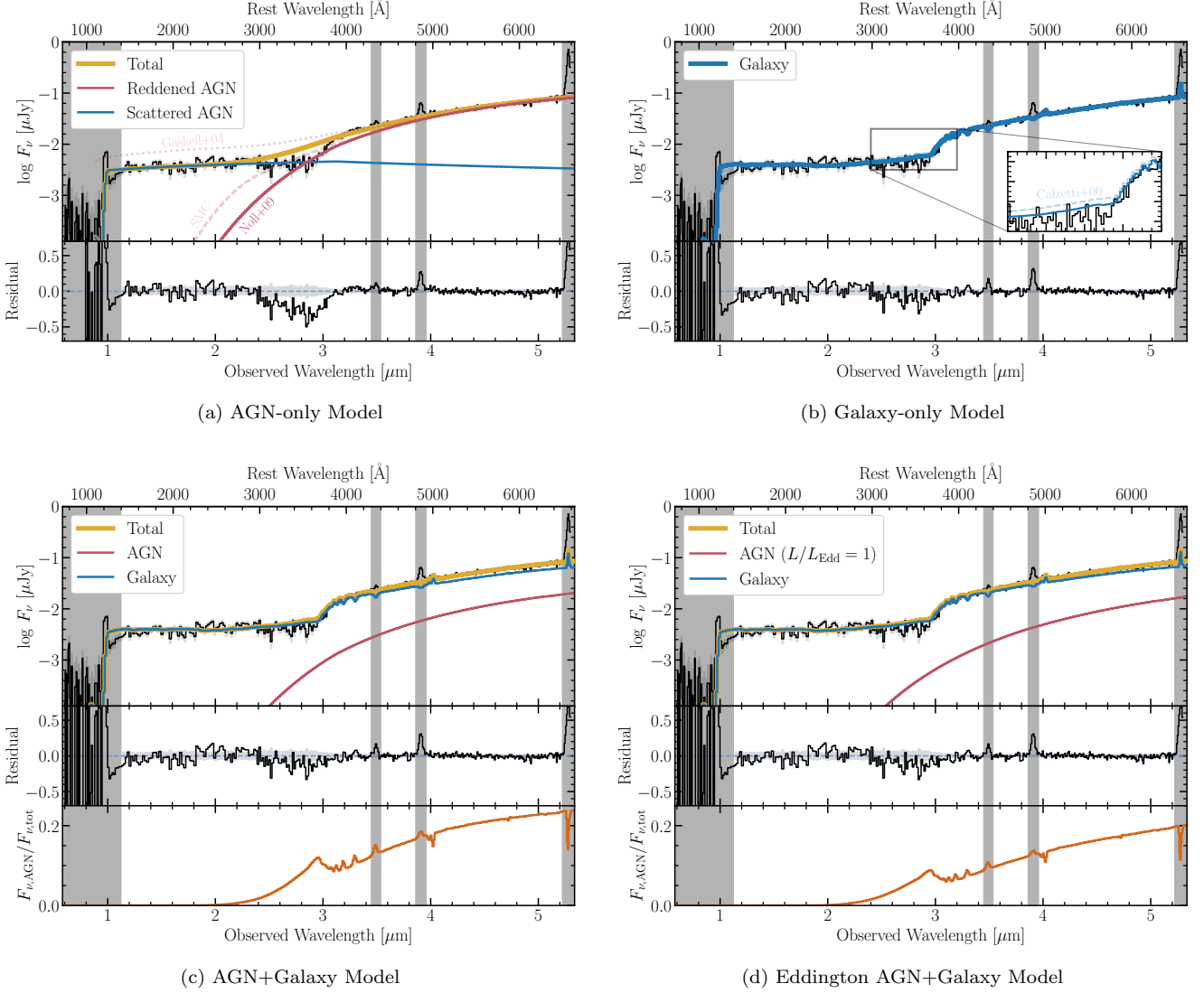
Parameter	Unit	AGN-only	Galaxy-only	AGN+Galaxy	EAGN+Galaxy
$\chi_\nu^2$	—	4.32	2.74	2.81	2.85
$\log M_*$	$M_\odot$	...	$9.71^{+0.03}_{-0.03}$	$9.56^{+0.02}_{-0.03}$	$9.59^{+0.02}_{-0.03}$
$\log \tau$	Gyr	...	$-1.94^{+0.05}_{-0.05}$	$-1.88^{+0.02}_{-0.03}$	$-1.88^{+0.02}_{-0.03}$
$t_{\text{start}}$	Gyr	...	$0.64^{+0.01}_{-0.01}$	$0.63^{+0.01}_{-0.01}$	$0.63^{+0.01}_{-0.01}$
$A_V^{\text{gal}}$	mag	...	$2.12^{+0.02}_{-0.02}$	$2.02^{+0.02}_{-0.02}$	$2.00^{+0.01}_{-0.02}$
$\delta$	—	< -1	< -1	< -1	< -1
$f_{\text{nodust}}$	%	...	$1.85^{+0.12}_{-0.09}$	$2.84^{+0.12}_{-0.10}$	$2.67^{+0.09}_{-0.09}$
$\log \lambda L_{\lambda,3000}$	$\text{erg s}^{-1}$	$44.42^{+0.02}_{-0.02}$	...	$43.99^{+0.03}_{-0.03}$	...
$A_V^{\text{AGN}}$	mag	$2.08^{+0.01}_{-0.01}$	...	$0.50^{+0.09}_{-0.09}$	$0.19^{+0.09}_{-0.08}$
$f_{\text{scat}}$	—	$1.13^{+0.02}_{-0.02}$	...	...	...
$\log M_{\text{BH}}$	$M_\odot$	$\dagger 7.60^{+0.18}_{-0.12}$	$\dagger 7.60^{+0.18}_{-0.12}$	$\dagger 7.60^{+0.18}_{-0.12}$	$6.17^{+0.03}_{-0.03}$

NOTE—The best-fit parameters and their uncertainties are presented. Any entry with “...” means the parameter is not involved in the modeling. The limit on the dust law slope  $\delta$  indicates that the parameter is pushing against the prior boundaries. We use “†” to mark out the BH masses inferred by [Furtak et al. \(2024\)](#) using standard emission line scaling relations.

continuum and the UV flux to unobscured, scattered light from the AGN.

We adopt the broken power law continuum empirically derived by [Temple et al. \(2021\)](#) from a population of type-1 quasars at  $0 < z < 5$  to be the intrinsic continuum of the AGN. Following the parametrization of [Temple et al. \(2021\)](#), the scaling of the continuum level is controlled by the unextincted luminosity at rest-frame 3000 Å,  $\lambda L_{\lambda,3000}$ . The continuum is then reddened using

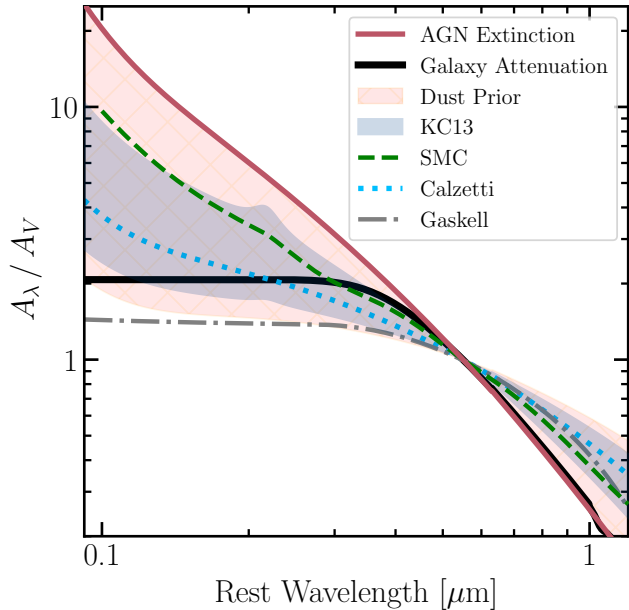
the [Noll et al. \(2009\)](#) curve parameterized by  $A_V$  and a multiplicative power law slope  $\delta$ . Given that the AGN is only observed along a single line of sight, it is true that an extinction curve instead of an attenuation curve is more appropriate in the modeling. Yet, this parameterization we choose is flexible enough to cover slopes ranging from a [Calzetti et al. \(2000\)](#) extinction law to the steep SMC curve ([Gordon et al. 2003](#)). Since the dust physics is still uncertain at such high redshift, we



**Figure 2.** The best-fit models for the four different scenarios proposed in this work. We plot the de-magnified spectra here. The solid red curve in each panel represents the reddened AGN continuum assuming the [Noll et al. \(2009\)](#) dust law. The dashed red curves in the AGN-only model are the best-fit reddened AGN component assuming the SMC dust law ([Gordon et al. 2003](#)) and the [Gaskell et al. \(2004\)](#) gray extinction law. The solid blue curves are starlight from the galaxy except in the AGN-only model, in which it represents the scattered unattenuated AGN continuum. The vertical bands are wavelength ranges that are masked in the fitting procedures. The dashed blue curve in the galaxy-only model is the best-fit assuming a [Calzetti et al. \(2000\)](#) dust law. For the two AGN+galaxy composite models, we also show the fraction of AGN contribution to the total continuum model as a function of wavelength in a third panel as the orange curve.

adopt a broad prior on the dust law slopes ( $\delta \in [-1, 0.4]$ , also see [Table 1](#)) such that gray extinction curves (i.e., smaller  $A_{UV}/A_V$ ) and dust laws steeper than that of SMC can be sampled. The scattered UV continuum is modeled as the unobscured AGN continuum scaled down by the scattering fraction  $f_{\text{scat}}$ . This AGN-only model includes four free parameters: the intrinsic luminosity  $\lambda L_{3000}$ , the scattering fraction  $f_{\text{scat}}$ , the dust reddening  $A_V$ , and dust law slope  $\delta$ .

We show in [Figure 2a](#) that the best-fit AGN-only model in this scenario does not reproduce the observed spectral shape well with a reduced chi-square value of  $\chi_\nu = 4.27$ . The summation of the reddened continuum and the scattered intrinsic power law produces a transition that is too smooth to fit the data around rest-frame  $3600 \text{ \AA}$ , i.e., the model overproduces flux at the break. We note that the dust law slope is pushing against the prior range (see [Table 2](#)), suppressing the UV flux as much as allowed. It is also steeper than that of the



**Figure 3.** The various dust attenuation laws are presented. The dark blue shaded area shows the dust law ranges empirically measured by Kriek et al. (2008). The red hatched shade shows the dust law priors in the fitting procedures. The solid curve (red) is the dust extinction law and the effective galaxy attenuation law (black) that the fits prefer, where the former also pushes against the prior boundary.

Small Magellanic Cloud (SMC), which is well suited to describe extinction in more typical AGN (e.g., Hopkins et al. 2004). In fact, when we use the SMC extinction law to fit the data, the reddened AGN component already overproduces flux at the break, as we show with a dashed curve in Figure 2a.

Therefore, we disfavor such an AGN-only model even though it is preferred for the photometric SED (Furtak et al. 2023a), because the combination of an unobscured power law and a reddened one cannot reproduce the strong break well, a feature that is only revealed with the addition of spectroscopy. It is possible that either stellar light contributes to the continuum in addition to the AGN hinted by the broad Balmer lines, or that the intrinsic AGN continuum and/or dust extinction curve of A2744-QSO1 does not resemble those of typical AGNs.

### 3.3. Galaxy-Only Model

Given that the AGN-only model fails to reproduce the observed break strength, we next seek models that produce strong breaks. The break feature has been associated with a Balmer break (Wang et al. 2024a,b), where it has been found that a galaxy-only model produces a statistically acceptable fit to the continuum. Thus, we naturally ask the question whether the continuum of

A2744-QSO1 is solely produced by galaxy light, which could easily show a Balmer break in the spectra.

We generate the galaxy SED with the flexible stellar population synthesis code (FSPS; Conroy et al. 2009; Conroy & Gunn 2010) using the MIST isochrones (Dotter 2016; Choi et al. 2016) and the MILES library of stellar spectrum templates (Sánchez-Blázquez et al. 2006; Falcón-Barroso et al. 2011). We also assume a simple delayed- $\tau$  star formation history, parameterized by the  $e$ -folding timescale  $\tau$  and the starting time  $t_{\text{start}}$ , and a Chabrier (2003) initial mass function (IMF). The nebular continuum is also included using the modeling by Byler et al. (2017) to account for the potential recombination and two-photon continua present in the UV wavelengths. Other weak nebular lines may also contribute to the model flux given the PRISM resolution, particularly at the break region. We assume a stellar metallicity  $\log(Z/Z_{\odot}) = -1$  to reflect the limited time available for multiple episodes of chemical enrichment in the first billion years after the Big Bang. This is supported by previous modeling; Wang et al. (2024a,b) infer similar stellar metallicities for other LRD-like objects at similar and lower redshifts using a similar setup as ours. Gallazzi et al. (2005) also indicates  $-1 \lesssim \log(Z/Z_{\odot}) \lesssim -0.5$  for local galaxies with stellar mass between  $10^9 M_{\odot}$  and  $10^{10} M_{\odot}$ , which turns out to be our estimate, too (see discussion below). The extremely weak metal emission lines in A2744-QSO1 that hint of low gas-phase metallicity also resonates with this assumed low stellar metallicity. We choose the dust law to be in the form of the Noll et al. (2009) curve. Lastly, we always allow a fraction of the stars to be entirely unattenuated — this is parameterized by  $f_{\text{nodust}} \equiv M_{\star, A_V=0}/M_{\star}$ , where  $M_{\star}$  is the total stellar mass. In total, this model consists of six free parameters:  $M_{\star}$ ,  $\tau$ ,  $t_{\text{start}}$ ,  $A_V^{\text{gal}}$ ,  $\delta$ , and  $f_{\text{nodust}}$ ; their respective priors are presented in Table 1.

We present the best-fit galaxy-only model in the top right panel of Figure 2b and the best-fit parameters in Table 2. If the entire continuum were to originate from stellar light, it would require a heavily reddened stellar population. The recent starburst has formed virtually all of the observed stellar mass ( $t_{\text{age}} \approx 100$  Myr and  $\tau \approx 10$  Myr) in this model. The galaxy would also be quite massive ( $M_{\star} \approx 5 \times 10^9 M_{\odot}$ ), which, when combined with its compact size of  $r_e < 30$  pc, implies a value that is a factor of five or larger than the upper limit on stellar mass derived in Furtak et al. (2024) assuming the empirical maximum stellar density (Baggen et al. 2023; Vanzella et al. 2023). Furthermore, in order for the stellar light not to overproduce any flux in the break, the dust law is required to be steeper than the Calzetti et al. (2000) and SMC curves and pushes against the prior



boundary. We show in the inset of Figure 2b that indeed, a grayer Calzetti et al. (2000) dust law does not produce the break strength as well as our steep dust law does. We note that models with more free parameters that assume a non-parametric star formation history are still unable to reproduce the break without a steep dust law (B. Wang, priv. comm., 2024), suggesting that our results are not sensitive to our choice of star formation history. However, since there is an unattenuated stellar component responsible for the UV continuum, although the underlying extinction law is steep ( $A_{1500}/A_V \approx 9.4$ ), the effective attenuation law to the stellar population only has a UV-optical slope of  $A_{1500}/A_V \approx 2.1$  taking into account the unobscured stars (see Figure 3). This UV-optical slope is not surprising for an object at optical attenuation of  $A_V \approx 2$  and consistent with the trend found at low redshift where attenuation laws are grayer (flatter slope between UV and optical) at higher  $A_V$  (Salim & Narayanan 2020). The phenomenon can be attributed to partially unobscured UV flux ranging from simple prescriptions as used in our model to more complex star-dust geometries (e.g., Narayanan et al. 2018; Salim & Narayanan 2020; Trayford et al. 2020).

Both the steep extinction law and the high stellar density may hint at the improbability of this model. Yet, nullifying the model requires stronger evidence. The fact that we have not seen objects with such high densities and/or steep dust law slopes does not mean they do not exist. Another significant challenge that the galaxy-only model faces is the deficiency of ionizing photons to produce the observed  $H\alpha$  luminosity. We first de-redden the best-fit galaxy-only model and remove the IGM absorption from the model. We then convert the number of photons between rest-frame 10 Å and 912 Å in the intrinsic (unattenuated) galaxy SED into an  $H\alpha$  luminosity assuming case-B recombination (Osterbrock & Ferland 2006). This fiducial  $H\alpha$  luminosity computed from the best-fit galaxy-only model is  $\sim 100$  times smaller than the observed value measured by Furtak et al. (2024) even without applying a reddening correction to the line luminosity. The presence of an AGN, as implied by the broad lines, would likely be required for the addition of more ionizing photons. Nonetheless, it is plausible to achieve high  $L_{H\alpha}$  with an O-star-dominated stellar population, but such a galaxy SED would contradict the observed strong Balmer break, which necessitates late-B and A-type stars within our modeling scheme. Beyond our setup, it is possible that the Balmer break has a non-stellar origin (e.g., Inayoshi & Maiolino 2024), and we discuss this possibility in Section 4.3. Therefore, given the challenges faced by this galaxy-only model, we conclude that the presence of an AGN is nearly inevitable.

### 3.4. AGN + Galaxy Model

Perhaps a more sensible and appropriately flexible model would include both the AGN and the galaxy. This would be a natural choice, given the strong break and the broad Balmer lines. Such a composite model has been shown to fit the data of other LRDs (and LRD-like objects) with Balmer breaks (Wang et al. 2024a,b). In addition, the AGN could also serve as a reservoir of ionizing photons to produce the observed  $H\alpha$  luminosity.

We model the galaxy as described in Section 3.3. The AGN is also modeled as in Section 3.2 using the empirical Temple et al. (2021) SED. In this composite model, the scattered light component is replaced with unobscured stellar light, although we stress that the UV origin still remains ambiguous. Both scattered AGN/galaxy light and unobscured star formation remain open possibilities (e.g., Killi et al. 2023; Labbe et al. 2023; Greene et al. 2024; Matthee et al. 2024) as we already demonstrate in the AGN-only and galaxy-only models. Adding any additional components in the UV would yield significant degeneracy in the fitting process as the UV slope due to star formation and that of an AGN is very similar (Greene et al. 2024). The AGN continuum is also reddened by galactic dust ( $A_V^{\text{gal}}$ ) in addition to its own circumnuclear dust ( $A_V^{\text{AGN}}$ ), i.e.  $A_{V,\text{tot}}^{\text{AGN}} = A_V^{\text{AGN}} + A_V^{\text{gal}}$ . For simplicity in the model, we assume that the AGN and the galaxy share the same dust law slope. The model is similar to Wang et al. (2024a), who model an LRD at  $z \approx 3$ , although the authors use two different dust laws and a non-parametric star formation history in their analysis. This composite model includes eight free parameters: the stellar mass  $M_*$ ,  $e$ -folding timescale  $\tau$  of star formation, starting time  $t_{\text{start}}$  of star formation, galaxy reddening  $A_V^{\text{gal}}$ , AGN luminosity  $\lambda L_{\lambda,3000}$ , AGN dust extinction  $A_V^{\text{AGN}}$ , and dust law slope  $\delta$ , and the fraction  $f_{\text{nodust}}$  of stars that are unobscured by dust. We show the best-fit parameters in Table 2 and discuss them in the following.

As shown in Figure 2c, the best-fit model in the AGN+Galaxy scenario is consistent with a galaxy-dominated continuum, which is quite similar to the galaxy-only model described in Section 3.3, but explains the discrepant  $H\alpha$  emission. The UV flux is entirely attributed to unobscured stellar light. A dusty 100-Myr-old galaxy is responsible for producing the observed break and most of the optical continuum, similar to the galaxy-only model described earlier. The reddened AGN only starts to contribute non-negligibly to the continuum emission redward of  $\lambda_{\text{rest}} \approx 5000$  Å but never dominates anywhere in the NIRSpc coverage. However, this model does predict an extinguished  $H\alpha$  luminosity that is a factor of  $\sim 2$  higher than the observed one. More-

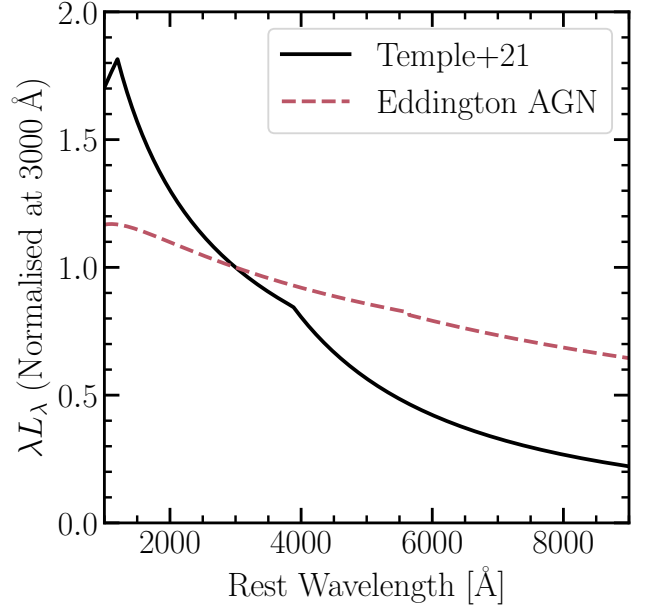
over, due to the AGN contribution in the rest-frame optical, the inferred stellar mass is lowered by a factor of  $\sim 1.5$  as listed in Table 2, but  $M_* \approx 4 \times 10^9 M_\odot$  is still rather massive for its compact size. We note that Balmer absorption lines are present in the model even at PRISM resolution, but observational noise and emission line infilling could easily wash out their presence in the observed spectrum.

While the joint model relieves some tension, the dust law slope remains steep and pushing against the prior such that the extinguished NUV photons from either the dust-obscured stars or the AGN do not wash out the break strength in the model. The dust law predicts a Balmer decrement of 11.4 for the broad line components, while the observed value is  $7.4 \pm 0.4$  using the combined broad and narrow emission line (Furtak et al. 2024). However, we stress that kinematic decomposition of the emission lines is challenging at the PRISM resolution (Greene et al. 2024), so the measured Balmer decrement does not necessarily reflect the true extinction experienced by the AGN due to contamination from the narrow-line components. Since the steep extinction law slope is already in place in the galaxy-only fit, and given the AGN+galaxy model is also galaxy-dominated, the steep extinction law for the AGN is possibly inherited from there. Of course, there is no reason a priori that the AGN and galaxy should share the same shape for their underlying extinction/attenuation laws; we will further discuss other extinction curves in Section 4.2.

Regardless, the failure of our AGN-only model in Section 3.2 already shows that if the AGN were to dominate anywhere in the optical continuum of A2744-QSO1, its extinction law would need to be as steep as our prior allows, if not more (i.e.  $\delta < -1$  or  $A_{1500}/A_V \gtrsim 9$ ; also see Figure 2a). This is necessary for the reddened continuum to drop fast enough to preserve the break strength. Otherwise, any grayer dust extinction curve would lead to a less extinguished UV continuum and force the AGN to be even more sub-dominant to preserve the break. In that case, we would once again face the deficiency of ionizing photons to explain the broad line luminosities as well as high equivalent width of the broad lines, because the fit would approach a galaxy-only one.

### 3.5. Eddington AGN + Galaxy Model

The previous AGN+galaxy model works well, but it still requires uncomfortably high mean stellar density and steep extinction slope. This is because the continuum is mostly dominated by galaxy and both the reddened stellar population and the AGN must not over-produce flux near  $\sim 3000 \text{ \AA}$ . It is possible that an intrinsically redder AGN continuum could alleviate the steep-



**Figure 4.** The two AGN SEDs are compared in this figure. The solid black curve is the empirical SED from type-1 quasars from SDSS obtained by Temple et al. (2021). The red dashed curve is an AGN SED with assumed  $L_{\text{bol}}/L_{\text{Edd}} = 1$  and  $M_{\text{BH}} = 10^{6.22} M_\odot$ .

ness of the dust law while allowing the AGN to dominate at redder wavelengths, thus lowering the stellar mass. AGNs with high Eddington ratios then become great candidates to naturally provide a intrinsically redder continuum when compared to typical AGNs accreting at sub-Eddington luminosities (Volonteri et al. 2017; Kubota & Done 2019). Furtak et al. (2024) suggest that A2744-QSO1 is one such BH with a high Eddington ratio. By adopting a BH mass of  $10^{7.3} M_\odot$  measured from the emission lines and scaling relations, the authors conclude that A2744-QSO1 is accreting at 30% of Eddington luminosity. The X-ray non-detections of LRDs (Akims et al. 2024; Yue et al. 2024), including A2744-QSO1 with a  $2\sigma$  upper limit of  $L_{2-10 \text{ keV}} < 10^{43.68} \text{ erg s}^{-1}$  (Ananna et al. 2024), is another line of evidence. Both numerical simulations and observations at lower redshifts have shown that AGNs and quasars accreting at high fractions of the Eddington limit could become X-ray weak (Ma et al. 2024; Pacucci & Narayan 2024) due to a lack of hot gas to up-scatter the UV photons and/or the disk photosphere obscuring the X-ray emitting region (Jiang et al. 2013). Greene et al. (2024) also suggest that near- or super-Eddington accretion rates may help explain the high number density of the LRD population.

Motivated by these points and the need for an intrinsically red continuum to preserve the break, we adopt the AGN SED from Volonteri et al. (2017). Their model is

inspired by the [Shakura & Sunyaev \(1973\)](#) disk solution and parameterized by the BH mass  $M_{\text{BH}}$  and Eddington ratio  $L_{\text{bol}}/L_{\text{Edd}}$ . Under this parameterisation, the peak position of the big blue bump as well as the UV-optical slope are variable: the SED assumes the peak temperature scaling from [Thomas et al. \(2016\)](#), normalizing the free parameters to obtain a good match with quasar bolometric corrections in the relevant luminosity and  $M_{\text{BH}}$  range. For this exercise, we have further modified the SED to have a redder intrinsic SED when the Eddington ratio is high, mimicking the effect of radiation trapping in super-Eddington sources ([Begelman 1979](#)). This is achieved by increasing the radius corresponding to the peak temperature. Since it is uncertain whether local scaling relations can be applied at high redshift, the previously measured BH mass and the Eddington ratio of A2744-QSO1 ([Furtak et al. 2024](#)) may not accurately reflect reality. We therefore assume that A2744-QSO1 is Eddington-limited ( $L_{\text{bol}}/L_{\text{Edd}} = 1$ ) in this exercise to break the degeneracy in the modeling when both  $M_{\text{BH}}$  and  $L_{\text{bol}}/L_{\text{Edd}}$  are set free, since both are involved in scaling the full spectrum. The goal is to test whether a redder (physically motivated) AGN continuum than [Temple et al. \(2021\)](#) could alleviate the steep dust law problem and have AGN dominate the rest-frame optical flux. We show the comparison between the two SEDs in [Figure 4](#). Except for the intrinsic AGN SED, the setup is the same as described in [Section 3.4](#). The model also totals 8 parameters, whose best-fit values are presented in [Table 2](#).

We show in [Figure 2d](#) that qualitatively, this setup yields the same model as the regular AGN+Galaxy setup, where the entire UV-optical continuum is dominated by a massive dust-reddened post-starburst galaxy, and the AGN is subdominant across all wavelengths. The fit also measures a BH mass is nearly 1 dex lower than the estimation from scaling relations. We note that since the size of the broad line region may change at high Eddington ratio (e.g., [Lupi et al. 2024](#)), BH masses estimated from emission line scalings may not be accurate. Furthermore, given that the best-fit model in this case is still galaxy-dominated and given our ignorance of the intrinsic SED of the AGN, our derived BH properties should be taken with a grain of salt. This model involving the Eddington-limited AGN is virtually indistinguishable from the regular AGN+galaxy model. The steep-dust-slope challenge is not alleviated by the redder AGN model, either; the best-fit remains galaxy-dominated, and the steepness of the dust law is necessary to preserve the strong break strength, just as in the galaxy-only model described in [Section 3.3](#). More importantly, the extinguished  $\text{H}\alpha$  luminosity predicted by

this Eddington AGN+galaxy model is roughly half of observed value. Since this model also under-supplies the photon budget needed to explain the high  $L_{\text{H}\alpha}$  of A2744-QSO1, we disfavor this model as well.

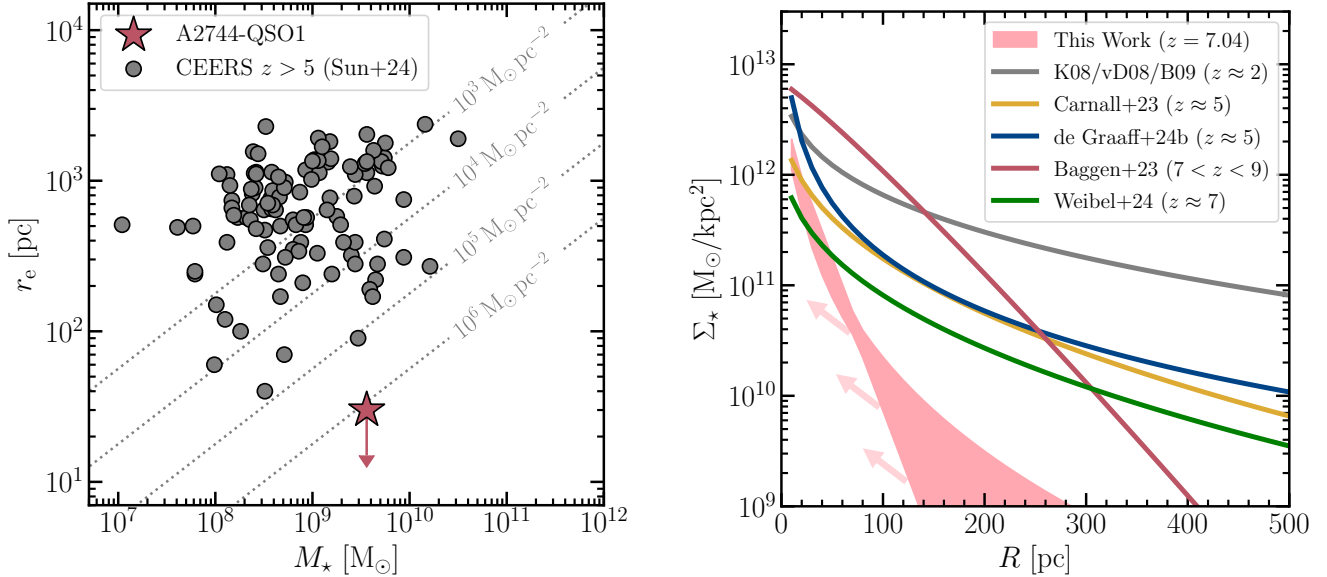
#### 4. DISCUSSION

We have presented four different options to describe the continuum emission of A2744-QSO1 in the previous section. The AGN-only model fails to produce the strong Balmer break feature and is therefore disfavored. The galaxy-only model and Eddington AGN+galaxy model yield reasonable fits to the continuum shape but do not provide enough UV photons to ionize the ISM to produce the observed broad line luminosity — for this reason, these models are also unsatisfactory. We therefore take the regular AGN+Galaxy model to be the fiducial model, where the UV-optical continuum is dominated by a massive post-starburst galaxy and the reddened AGN begins to contribute non-negligibly redward of  $\text{H}\beta$ .

Nonetheless, challenges still exist in this composite model. The best-fit stellar mass is so large compared to A2744-QSO1’s compact size that the derived stellar surface density is among the largest seen in current observations. Also, in order for the model to not over-produce flux just blueward of the break, dust extinction laws steeper than that of the SMC are required. Furthermore, given these challenges, the most likely scenario is that we are missing some physical elements in all of our modeling. In this section, we discuss some of these issues and the implications of galaxy and BH growth below.

##### 4.1. Galaxy and BH Properties

We first discuss the galaxy and BH properties taking our fiducial AGN+galaxy model at face value. This composite model infers a stellar mass of  $\sim 4 \times 10^9 M_{\odot}$  within an extremely small effective radius of 30 pc, comparable to the size of a star cluster. We show in the left panel of [Figure 5](#) that this corresponds to  $\langle \Sigma_{\star} \rangle \approx 10^6 M_{\odot} \text{pc}^{-2}$  and is among the densest in a sample of high-redshift systems. In this fit, all UV light originates from the galaxy; if AGN were to contribute in the UV, the inferred stellar density would be reduced. However, although the average density seems extreme, we show on the right panel of the same figure that the central density (assuming Sérsic index  $n = 1$  to  $n = 4$ ) of A2744-QSO1 is similar to but does not exceed the high central density found in many other compact massive quiescent galaxies at  $z \gtrsim 5$  ([Carnall et al. 2023](#); [de Graaff et al. 2024b](#)). Compact massive quiescent galaxies have been found at lower redshift as well (e.g., [van Dokkum et al. 2008](#); [Szomoru et al. 2012](#); [Wright et al. 2024](#)). These



**Figure 5.** **Left:** The stellar mass and size of A2744-QSO1 (red star) is plotted against a sample of  $z > 5$  galaxies (Sun et al. 2024) represented by the gray circles. The dashed lines are lines of constant surface mass density. **Right:** The assumed density profile of A2744-QSO1 (range due to assuming  $n = 1$  and  $n = 4$ ) is compared against other compact objects at various redshifts (van Dokkum et al. 2008, see also Kriek et al. 2008 and Bezanson et al. 2009); Baggen et al. 2023; Carnall et al. 2023; de Graaff et al. 2024b; Weibel et al. 2024) using the  $r_e = 30$  pc upper limit. The arrows represent the direction of the changes in the curve assuming sizes smaller than 30 pc.

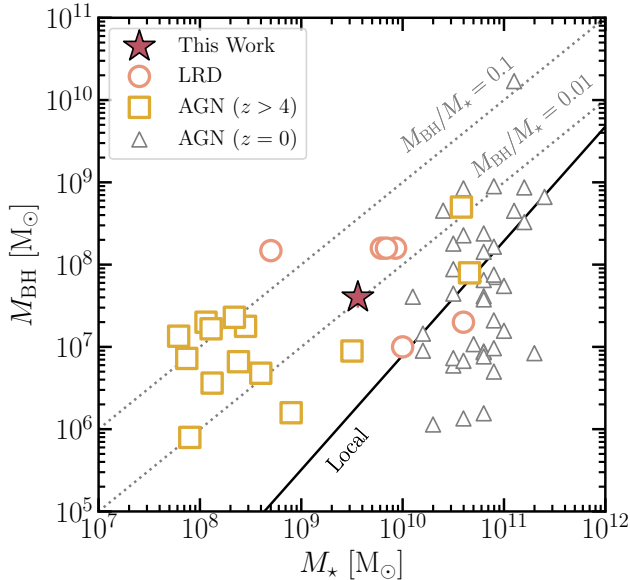
galaxies tend to show an extended wing on scales of  $\gtrsim 200$  pc in their density profile due to the high Sérsic indices (see the  $z \approx 2$  curve in Figure 5 as an example) when compared with our 30 pc-object. We may thus picture their predecessors to be objects like A2744-QSO1 that later grow by minor mergers in the outskirts of the systems (Bezanson et al. 2009; Naab et al. 2009; van Dokkum et al. 2010; Newman et al. 2013; Suess et al. 2023). This scenario is particularly plausible given that some LRDs show a preference for overdense regions (Lin et al. 2024; Labbé et al. in prep.). We mention that observations with adaptive optics on future 20-30m level ground-based telescopes could potentially resolve such a compact morphology and provide more insight on the light profile of LRDs.

Moreover, A2744-QSO1 also has one of the strongest breaks observed at  $z \gtrsim 5$  even when other LRDs are included. Weibel et al. (2024) measure a Balmer break strength of  $3.33 \pm 0.15$  for the A2744-QSO1, as defined by Wang et al. (2024a) to be the ratio of the median fluxes in rest-frame 3620–3630 Å and 4000–4100 Å. In order to reproduce the strong break, our model necessitates the galaxy host of A2744-QSO1 to be an A-star-dominated massive post-starburst galaxy with all of its stellar population forming nearly simultaneously. Such a star formation history on a star cluster size scale would require

that feedback from supernova explosions does not kick in and disrupt this intense starburst. Indeed, Dekel et al. (2023) propose that massive galaxies can efficiently form via feedback-free starbursts if the metallicity is low and the gas density is high, which seems to be the suitable regime for A2744-QSO1.

We now focus on the BH in A2744-QSO1, which we estimate to have a luminosity of  $\lambda L_{\lambda, 3000} \approx 10^{44}$  erg s $^{-1}$  in our fiducial model. Taking  $M_{\text{BH}} = 4 \times 10^7 M_{\odot}$  derived from the H $\alpha$  emission line (Furtak et al. 2024), we show in Figure 6 that our fiducial model yields  $M_{\text{BH}}/M_{\star} \approx 1\%$ . This ratio is consistent with other LRDs with estimates for both masses. Like many high- $z$  AGN (e.g. Maiolino et al. 2023), the BH in A2744-QSO1 is overmassive compared to the local population (Greene et al. 2020). Comparably extreme  $M_{\text{BH}}/M_{\star}$  have been observed before, even locally as we show in Figure 6. These extreme ratios could reflect an evolution in the intrinsic  $M_{\text{BH}}-M_{\star}$  relation, but it is also possible that these overmassive BHs in LRDs only represent the scatter in a redshift-invariant scaling relation due to selection biases and measurement uncertainties (Lauer et al. 2007; Li et al. 2024a). The latter is especially feasible given that some LRDs do fall onto the local relation (Fujimoto et al. 2022; Kokorev et al. 2023). Alternatively, tidal stripping in overdense environment, which

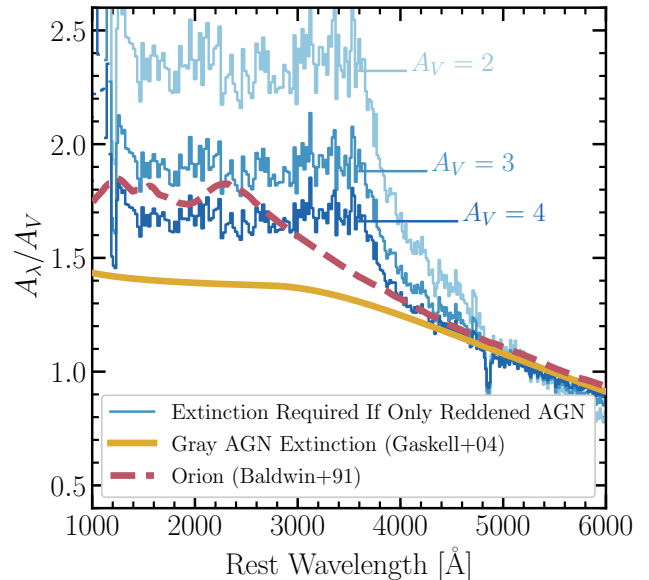




**Figure 6.** The stellar mass and BH mass of A2744-QSO1 is plotted against various samples. The BH mass of A2744-QSO1 is taken from Furtak et al. (2024) since our inferred  $M_{\text{BH}}$  from the Eddington AGN+galaxy model assumes  $L/L_{\text{Edd}} = 1$  and is highly uncertain and systematics-dominated. The solid star shows our measurement of the stellar mass from our fiducial AGN+Galaxy model. The circles are LRDs from Fujimoto et al. (2022), Kokorev et al. (2023), Wang et al. (2024b), and Kokorev et al. (2024b). The high- $z$  AGN comparison sample are the yellow squares and are from Carnall et al. (2023), Larson et al. (2023), Maiolino et al. (2023), Chisholm et al. (2024), Juodžbalis et al. (2024), and Maiolino et al. (2024b). The local comparison sample (gray triangles) and scaling relation (solid black line) are from Greene et al. (2020).

the LRDs prefer as we mentioned before, could also result in both compact morphology and overmassive BHs (Volonteri et al. 2008; Barber et al. 2016; Vogel et al. 2019).

The high black-hole-to-galaxy mass ratio of A2744-QSO1 and the LRD population (e.g., Kokorev et al. 2023; Wang et al. 2024b) may shed light on seeding mechanisms of early BHs, especially given their high number density at  $z \gtrsim 4$  (Pacucci et al. 2023). Furthermore, given the compact size and the consequently implied high stellar density of A2744-QSO1, seeding mechanisms in high-density environments would be relevant (e.g., Devecchi & Volonteri 2009; Alexander & Natarajan 2014; Reinoso et al. 2023; Dayal 2024). However, we re-iterate here that considering the inability of our model to resolve issues like the dust law and the validity of local scaling relations at high redshift, the BH and galaxy masses must be taken with a grain of salt. As shown in the Eddington AGN+Galaxy fit, the AGN



**Figure 7.** The empirical extinction laws (shown in blue) one would obtain if the entire UV-optical continuum of A2744-QSO1 were dominated by a reddened AGN power law is compared against the gray (Gaskell et al. 2004) extinction curve (yellow solid curve) and the extinction curve found in the Orion Nebula (red dashed curve; Baldwin et al. 1991). The different shades of blue represent different levels of assumed extinction.

continuum could be entirely buried beneath the galaxy. This scenario leads to a smaller BH mass and larger galaxy mass, and would bring the mass ratio even closer to the local relation as well.

#### 4.2. The Role of Dust

In addition to the high stellar density of A2744-QSO1, another uncomfortable component of the fiducial model is the necessity for both the AGN and galaxy to have a steep dust law beyond the SMC one, as shown in Figure 3 and discussed in Section 3.2 and 3.4. We stress here that the UV flattening in the effective galaxy attenuation curve in Figure 3 only reflects our choice to model the UV emission as unobscured stellar light; if we were to use the AGN scattered light to describe the UV, this effective attenuation law would not show such a flattening behaviour. Regardless how we model the UV, the required dust law redward of the break, which is independent of this imposed star-dust geometry, is inferred to be quite steep as well. This steepness is strictly required such that the summation of the reddened galaxy/AGN component in the optical and the unobscured component in the UV preserves the strong break. We first discuss the steepness under the context of our modeling framework, and then discuss whether any other dust ex-



extinction laws beyond our modeling scheme could explain the spectral shape of A2744-QSO1.

A steep dust extinction curve could be due to a size distribution tilted towards small grains. Naïvely, our finding is consistent with the simple picture that lower metallicity environments lead to steeper dust laws, echoing the weak metal emission lines in the observed spectrum. Since dust grains tend to be smaller when metallicity is low, they lead to more extinction at shorter wavelengths and hence steepen the extinction curve, as we observe in the SMC (Gordon et al. 2003; Dubois et al. 2024). In addition, large grains may be preferentially destroyed by supernova and/or AGN shocks (Draine & Salpeter 1979; Jones et al. 1994), resulting in the steepening of the extinction law in AGN environments (e.g., Hall et al. 2002; Jiang et al. 2019). Given the compact size of A2744-QSO1, it is not hard for shocks from a few supernovae or the AGN itself, if any, to shape the dust properties of the entire system. Thus, the steep dust law could be explained physically by the grain size distribution.

It is also true that dust extinction laws with entirely different shapes beyond our parameterization do exist. For instance, gray extinction curves, which are usually flat at short wavelength (e.g., Maiolino et al. 2001; Czerny et al. 2004; Gaskell et al. 2004) usually found in composite AGN spectra have been invoked to explain V-shaped SED of LRDs (Killi et al. 2023; Li et al. 2024b). Killi et al. (2023) are able to model the NIR-Spec/PRISM spectrum of a  $z \approx 4.5$  LRD using the Gaskell et al. (2004) extinction curve, yielding an optical continuum dominated by a reddened AGN and a star-forming galaxy responsible for the UV flux. Seeking a more general model to explain the SED shape from NIRCcam and MIRI photometry, Li et al. (2024b) also utilize a gray extinction curve similar to that found in the Orion nebula (Baldwin et al. 1991) given the absence of small grains to explain the V-shaped SED and the flattening of the NIR flux. With this extinction curve, the authors claim that the UV-optical continuum of LRDs is entirely dominated by a dust-reddened AGN. However, we show in Figure 2a that the gray (Gaskell et al. 2004) extinction law entirely misses the shape of the strong break in A2744-QSO1. Moreover, we show in Figure 7 the dust extinction laws one would empirically infer from the data if the observed spectrum of A2744-QSO1 were entirely dominated by a reddened AGN power-law at different assumed values of  $A_V$ . The inferred three-sloped dust extinction curve would not resemble the two-sloped gray extinction law due to the break feature. Therefore, we do not consider the gray

extinction laws to be sufficient in explaining the V-shape of A2744-QSO1 and its strong break simultaneously.

Just as with the BH and galaxy masses, the dust law also has its own uncertainty — this may mark our ignorance of the dust properties in the LRDs and/or the early universe. The difficulty for our model to resolve the steepness of the dust law is also suggestive of the incompleteness of our model. Uncertainties in fitting the dust laws are exacerbated by our ignorance about the underlying continuum shape. However, although modeling photometric SED could be successful with a pre-chosen extinction curve, it is when spectroscopic data becomes available that modeling the break, particularly its strength, becomes challenging as is the case for A2744-QSO1 and other LRDs with similarly strong breaks (Wang et al. 2024a; Labbé et al. in prep.).

To further understand dust properties in A2744-QSO1 and the larger LRD population, it is crucial to obtain deeper and redder data from ALMA. Currently, ALMA observations of A2744-QSO1 yields no significant detection in the 1.2 mm continuum expected from the 20 K cold dust heated by stellar light with a  $3\sigma$  upper limit of 0.1 mJy (Labbe et al. 2023; Fujimoto et al. 2023; Furtak et al. 2024) — the prediction from our galaxy model exceeds this limit. Given the compact size of A2744-QSO1, hotter dust would reconcile the nondetection by shifting the peak of the dust thermal emission to shorter wavelengths (Casey et al. 2024). If deep observations covering rest-frame sub-millimeter wavelengths are available, we may be able to constrain the dust properties such as their temperature as well as the dust extinction expectations.

#### 4.3. Alternative Models

All of our discussion above is predicated on the assumption that some combination of the power-law AGN+galaxy+attenuation model can describe the truth. However, we should acknowledge the fact that we may not understand the physical origin of the spectral shape of A2744-QSO1, particularly given the resulting high stellar density and the required steep dust curves discussed in previous sections.

Under our scheme, the strong break necessitates an A-star-dominated stellar population, and the broad line luminosity and line width requires an AGN to photoionize the circumnuclear gas. Having AGN continuum explicitly present in the model also avoids the line equivalent width from reaching infinity (relative to the AGN continuum). However, as suggested by Maiolino et al. (2024a), the BLR clouds could be very compact and dense with a large covering factor around the accretion disk. Thus, it is possible that only the disk continuum

is obscured, and broad line emission gets out. In this case, we effectively have a galaxy-dominated continuum and the AGN produces broad lines with high equivalent widths. However, as noted by Kokubo & Harikane (2024), this geometry is rather contrived and does not match the high number density of LRDs based on variability studies of Sloan quasars (Sesar et al. 2007).

On this note, we re-explore the galaxy-only model, assuming an AGN is entirely absent. Particularly, Baggen et al. (2024) propose that the broad, high-luminosity Balmer emission lines present in LRDs’ spectrum may be achieved solely by stellar populations without an AGN. The authors point out that the broad line width may simply reflect the velocity dispersion of the ionized gas tracing the stellar distribution in such a compact dense system, and the presence of an AGN may not be needed. Indeed, if we take the 30 pc-upper limit on the effective radius and the stellar mass derived from our galaxy-only model at face value, we would obtain a lower limit of  $\text{FWHM} \gtrsim 1400 \text{ km s}^{-1}$  for the emission line width, consistent with the observed value for A2744-QSO1 (Furtak et al. 2024; Greene et al. 2024). Such high velocity dispersion may also provides an explanation for the lack of observed absorption features at the break region as the PRISM resolution could smear out these broad absorption lines, although observational noise and emission line infilling could already explain their absence and the smoothness of the observed spectrum as we mention in Section 3.3. Without photoionization from the AGN, the high  $L_{\text{H}\alpha}$  may also be achieved with shocks or collisional excitation in the potentially high-density gas due to the compact size of A2744-QSO1 (Draine & McKee 1993; Stasińska & Izotov 2001; Baggen et al. 2024, and references therein) although future modeling of these mechanisms is needed to confirm their viability. Moreover, a top-heavy initial mass function resulting in a stellar population favoring massive stars could provide sufficient ionizing photons (Schaerer et al. 2024; van Dokkum & Conroy 2024; Baggen et al. 2024, and references therein). Massive stars stripped of their envelopes in binaries may also provide sufficiently hard ionizing spectrum to reproduce the strong emission lines without significantly changing the SED shape redder than the Lyman break (Götberg et al. 2020).

It is also possible that the entire UV-optical continuum is dominated by an exotic AGN whose SED shape is not well characterized — this is particularly plausible given the potential high Eddington ratio of A2744-QSO1 and the entire LRD population. For instance, Thompson et al. (2005) provide a disk solution with accretion rate near the Eddington limit and whose disk scale height drops at the location of  $T \approx 10^4 \text{ K}$  because

of an opacity gap from hydrogen recombination at that temperature. Naturally, this scenario would result in a two-piece continuum (with appropriate dust reddening) because the inner and outer disk have different structures. Also, the strong break could be produced by continuous Balmer absorption by dense gas near the disk photosphere as well (Inayoshi & Maiolino 2024) — this is analogous to the star-like disk SED proposed by Laor & Davis (2011). Nonetheless, detailed modeling of the AGN SEDs with high Eddington ratios, similar to those down by Kubota & Done (2019), is required in the future in the context of LRDs.

Regardless of the exact shape of the intrinsic SED, if the continuum emission from A2744-QSO1 is dominated by an AGN, it should show signatures of variability on timescales of months to years in the rest frame. For sources like A2744-QSO1 that has three (or generally, multiple) gravitationally lensed images, every single epoch of observation corresponds to three (multiple) epochs in the rest-frame, making the light curve sampling much more efficient (Golubchik et al. 2024). If any variability signature is detected, this would confirm the AGN nature of A2744-QSO1 and enable reverberation mapping with *JWST* to obtain a more accurate and precise BH mass measurement. High-SNR medium- or high-resolution spectroscopy may reveal absorption lines in the break, thus confirming the stellar origin of the break (e.g., Kokorev et al. 2024b) without seeking for any non-traditional models to explain the full continuum shape.

## 5. SUMMARY

In this work, we conduct spectral decomposition of the NIRSpec/PRISM spectrum of the triply imaged A2744-QSO1, one of the first LRDs discovered by *JWST* (Furtak et al. 2023a, 2024) with a strong break feature at rest-frame 3600-4000 Å. Thanks to the strong magnification due to gravitational lensing of the foreground galaxy cluster, the spectrum we obtain has a high SNR of  $\sim 20$  per pixel, and its spectral shape can be confirmed by both the broad band and medium band photometry. The consistency of A2744-QSO1 being point-like across all three lensed images in all photometric bands allows us to set a firm size upper limit of  $r_e < 30 \text{ pc}$  for A2744-QSO1. In this light, we attempt to model the UV-optical SED and describe the peculiar spectral shape of A2744-QSO1 with a combination of AGN and stellar populations. Our fiducial model includes a composite of galaxy light that dominates the continuum and a significantly reddened AGN component that is entirely sub-dominant. However, the need to reproduce the strong break strength and the bright

emission lines leads us to a specific (contrived) combination of physical parameters, including an uncomfortably high stellar density and unusually steep extinction law. Therefore, we conclude that we do not find any model, including the fiducial one, to be fully satisfactory, and the true nature of A2744-QSO1 remains unconfirmed.

Our analysis demonstrates that while the observed spectral shape can be well reproduced by our models, many challenges to physically interpret the models are still present. In addition to the difference in the details of model setups, more generally, it is indeed true that we embark on a different approach from previous attempts of LRD modeling (e.g., Wang et al. 2024a,b) by trusting the shape of the continuum measurement given the high SNR. However, these emergent challenges to physically interpret the models are consistent across multiple approaches despite their differences. Thus, we encourage both theoretical modeling and deep long-wavelength follow-up observations for A2744-QSO1 (and the larger LRD population) to unveil their enigmatic nature.

#### ACKNOWLEDGEMENTS

This work is based in part on observations made with the NASA/ESA/CSA *James Webb Space Telescope*. The data presented in this work was obtained from the Mikulski Archive for Space Telescopes (MAST)

at the Space Telescope Science Institute (STScI), which is operated by the Association of Universities for Research in Astronomy, Inc., under NASA contract NAS 5-03127 for *JWST*. These observations are associated with *JWST* Cycle 1 GO program #2561 and Cycle 2 GO program #4111. The specific observations analyzed can be accessed at [10.17909/8k5c-xr27](https://doi.org/10.17909/8k5c-xr27). Support for program JWST-GO2561 was provided by NASA through a grant from the STScI, which is operated by the Associations of Universities for Research in Astronomy, Incorporated, under NASA contract NAS5-26555.

P.D. acknowledges support from the NWO grant 016.VIDI.189.162 (“ODIN”) and warmly thanks the European Commission’s and University of Groningen’s CO-FUND Rosalind Franklin program.

K.G. acknowledges support from Australian Research Council Laureate Fellowship FL180100060.

A.Z. acknowledges support by grant No. 2020750 from the United States-Israel Binational Science Foundation (BSF) and grant No. 2109066 from the United States National Science Foundation (NSF), by the Israel Science Foundation Grant No. 864/23, and by the Ministry of Science & Technology, Israel.

The work of CCW is supported by NOIRLab, which is managed by the Association of Universities for Research in Astronomy (AURA) under a cooperative agreement with the National Science Foundation.

#### REFERENCES

- Akins, H. B., Casey, C. M., Lambrides, E., et al. 2024, arXiv e-prints, arXiv:2406.10341, doi: [10.48550/arXiv.2406.10341](https://doi.org/10.48550/arXiv.2406.10341)
- Alexander, T., & Natarajan, P. 2014, *Science*, 345, 1330, doi: [10.1126/science.1251053](https://doi.org/10.1126/science.1251053)
- Ananna, T. T., Bogdán, Á., Kovács, O. E., Natarajan, P., & Hickox, R. C. 2024, arXiv e-prints, arXiv:2404.19010, doi: [10.48550/arXiv.2404.19010](https://doi.org/10.48550/arXiv.2404.19010)
- Baggen, J. F. W., van Dokkum, P., Labbé, I., et al. 2023, *ApJL*, 955, L12, doi: [10.3847/2041-8213/acf5ef](https://doi.org/10.3847/2041-8213/acf5ef)
- Baggen, J. F. W., van Dokkum, P., Brammer, G., et al. 2024, arXiv e-prints, arXiv:2408.07745, doi: [10.48550/arXiv.2408.07745](https://doi.org/10.48550/arXiv.2408.07745)
- Baldwin, J. A., Ferland, G. J., Martin, P. G., et al. 1991, *ApJ*, 374, 580, doi: [10.1086/170146](https://doi.org/10.1086/170146)
- Banerji, M., Alaghband-Zadeh, S., Hewett, P. C., & McMahon, R. G. 2015, *MNRAS*, 447, 3368, doi: [10.1093/mnras/stu2649](https://doi.org/10.1093/mnras/stu2649)
- Barber, C., Schaye, J., Bower, R. G., et al. 2016, *MNRAS*, 460, 1147, doi: [10.1093/mnras/stw1018](https://doi.org/10.1093/mnras/stw1018)
- Barro, G., Pérez-González, P. G., Kocevski, D. D., et al. 2024, *ApJ*, 963, 128, doi: [10.3847/1538-4357/ad167e](https://doi.org/10.3847/1538-4357/ad167e)
- Begelman, M. C. 1979, *MNRAS*, 187, 237, doi: [10.1093/mnras/187.2.237](https://doi.org/10.1093/mnras/187.2.237)
- Bezanson, R., van Dokkum, P. G., Tal, T., et al. 2009, *ApJ*, 697, 1290, doi: [10.1088/0004-637X/697/2/1290](https://doi.org/10.1088/0004-637X/697/2/1290)
- Bezanson, R., Labbe, I., Whitaker, K. E., et al. 2022, arXiv e-prints, arXiv:2212.04026, doi: [10.48550/arXiv.2212.04026](https://doi.org/10.48550/arXiv.2212.04026)
- Bouwens, R. J., Illingworth, G. D., Oesch, P. A., et al. 2015, *ApJ*, 803, 34, doi: [10.1088/0004-637X/803/1/34](https://doi.org/10.1088/0004-637X/803/1/34)
- Brammer, G. 2023a, msaexp: NIRSpec analysis tools, 0.6.17, Zenodo, doi: [10.5281/zenodo.7299500](https://doi.org/10.5281/zenodo.7299500)
- . 2023b, grizli, 1.9.11, Zenodo, doi: [10.5281/zenodo.1146904](https://doi.org/10.5281/zenodo.1146904)
- Buchner, J., Georgakakis, A., Nandra, K., et al. 2014, *A&A*, 564, A125, doi: [10.1051/0004-6361/201322971](https://doi.org/10.1051/0004-6361/201322971)
- Bushouse, H., Eisenhamer, J., Dencheva, N., et al. 2024, JWST Calibration Pipeline, 1.14.0, Zenodo, doi: [10.5281/zenodo.10870758](https://doi.org/10.5281/zenodo.10870758)

- Byler, N., Dalcanton, J. J., Conroy, C., & Johnson, B. D. 2017, *ApJ*, 840, 44, doi: [10.3847/1538-4357/aa6c66](https://doi.org/10.3847/1538-4357/aa6c66)
- Calzetti, D., Armus, L., Bohlin, R. C., et al. 2000, *ApJ*, 533, 682, doi: [10.1086/308692](https://doi.org/10.1086/308692)
- Cameron, A. J., Katz, H., Witten, C., et al. 2024, *MNRAS*, doi: [10.1093/mnras/stae1547](https://doi.org/10.1093/mnras/stae1547)
- Carnall, A. C., McLure, R. J., Dunlop, J. S., et al. 2023, *Nature*, 619, 716, doi: [10.1038/s41586-023-06158-6](https://doi.org/10.1038/s41586-023-06158-6)
- Casey, C. M., Akins, H. B., Kokorev, V., et al. 2024, arXiv e-prints, arXiv:2407.05094, doi: [10.48550/arXiv.2407.05094](https://doi.org/10.48550/arXiv.2407.05094)
- Chabrier, G. 2003, *PASP*, 115, 763, doi: [10.1086/376392](https://doi.org/10.1086/376392)
- Chisholm, J., Berg, D. A., Endsley, R., et al. 2024, arXiv e-prints, arXiv:2402.18643, doi: [10.48550/arXiv.2402.18643](https://doi.org/10.48550/arXiv.2402.18643)
- Choi, J., Dotter, A., Conroy, C., et al. 2016, *ApJ*, 823, 102, doi: [10.3847/0004-637X/823/2/102](https://doi.org/10.3847/0004-637X/823/2/102)
- Conroy, C., & Gunn, J. E. 2010, *ApJ*, 712, 833, doi: [10.1088/0004-637X/712/2/833](https://doi.org/10.1088/0004-637X/712/2/833)
- Conroy, C., Gunn, J. E., & White, M. 2009, *ApJ*, 699, 486, doi: [10.1088/0004-637X/699/1/486](https://doi.org/10.1088/0004-637X/699/1/486)
- Czerny, B., Li, J., Loska, Z., & Szczerba, R. 2004, *MNRAS*, 348, L54, doi: [10.1111/j.1365-2966.2004.07590.x](https://doi.org/10.1111/j.1365-2966.2004.07590.x)
- Dayal, P. 2024, arXiv e-prints, arXiv:2407.07162, doi: [10.48550/arXiv.2407.07162](https://doi.org/10.48550/arXiv.2407.07162)
- de Graaff, A., Rix, H.-W., Carniani, S., et al. 2024a, *A&A*, 684, A87, doi: [10.1051/0004-6361/202347755](https://doi.org/10.1051/0004-6361/202347755)
- de Graaff, A., Setton, D. J., Brammer, G., et al. 2024b, arXiv e-prints, arXiv:2404.05683, doi: [10.48550/arXiv.2404.05683](https://doi.org/10.48550/arXiv.2404.05683)
- Dekel, A., Sarkar, K. C., Birnboim, Y., Mandelker, N., & Li, Z. 2023, *MNRAS*, 523, 3201, doi: [10.1093/mnras/stad1557](https://doi.org/10.1093/mnras/stad1557)
- Devecchi, B., & Volonteri, M. 2009, *ApJ*, 694, 302, doi: [10.1088/0004-637X/694/1/302](https://doi.org/10.1088/0004-637X/694/1/302)
- Dotter, A. 2016, *ApJS*, 222, 8, doi: [10.3847/0067-0049/222/1/8](https://doi.org/10.3847/0067-0049/222/1/8)
- Draine, B. T., & McKee, C. F. 1993, *ARA&A*, 31, 373, doi: [10.1146/annurev.aa.31.090193.002105](https://doi.org/10.1146/annurev.aa.31.090193.002105)
- Draine, B. T., & Salpeter, E. E. 1979, *ApJ*, 231, 438, doi: [10.1086/157206](https://doi.org/10.1086/157206)
- Dubois, Y., Rodríguez Montero, F., Guerra, C., et al. 2024, *A&A*, 687, A240, doi: [10.1051/0004-6361/202449784](https://doi.org/10.1051/0004-6361/202449784)
- Falcón-Barroso, J., Sánchez-Blázquez, P., Vazdekis, A., et al. 2011, *A&A*, 532, A95, doi: [10.1051/0004-6361/201116842](https://doi.org/10.1051/0004-6361/201116842)
- Fan, X., Bañados, E., & Simcoe, R. A. 2023, *ARA&A*, 61, 373, doi: [10.1146/annurev-astro-052920-102455](https://doi.org/10.1146/annurev-astro-052920-102455)
- Fan, X., Narayanan, V. K., Lupton, R. H., et al. 2001, *AJ*, 122, 2833, doi: [10.1086/324111](https://doi.org/10.1086/324111)
- Feroz, F., & Hobson, M. P. 2008, *MNRAS*, 384, 449, doi: [10.1111/j.1365-2966.2007.12353.x](https://doi.org/10.1111/j.1365-2966.2007.12353.x)
- Feroz, F., Hobson, M. P., & Bridges, M. 2009, *MNRAS*, 398, 1601, doi: [10.1111/j.1365-2966.2009.14548.x](https://doi.org/10.1111/j.1365-2966.2009.14548.x)
- Feroz, F., Hobson, M. P., Cameron, E., & Pettitt, A. N. 2019, *The Open Journal of Astrophysics*, 2, 10, doi: [10.21105/astro.1306.2144](https://doi.org/10.21105/astro.1306.2144)
- Fujimoto, S., Brammer, G. B., Watson, D., et al. 2022, *Nature*, 604, 261, doi: [10.1038/s41586-022-04454-1](https://doi.org/10.1038/s41586-022-04454-1)
- Fujimoto, S., Bezanson, R., Labbe, I., et al. 2023, arXiv e-prints, arXiv:2309.07834, doi: [10.48550/arXiv.2309.07834](https://doi.org/10.48550/arXiv.2309.07834)
- Furtak, L. J., Zitrin, A., Plat, A., et al. 2023a, *ApJ*, 952, 142, doi: [10.3847/1538-4357/acdc9d](https://doi.org/10.3847/1538-4357/acdc9d)
- Furtak, L. J., Zitrin, A., Weaver, J. R., et al. 2023b, *MNRAS*, 523, 4568, doi: [10.1093/mnras/stad1627](https://doi.org/10.1093/mnras/stad1627)
- Furtak, L. J., Labbé, I., Zitrin, A., et al. 2024, *Nature*, 628, 57, doi: [10.1038/s41586-024-07184-8](https://doi.org/10.1038/s41586-024-07184-8)
- Gallazzi, A., Charlot, S., Brinchmann, J., White, S. D. M., & Tremonti, C. A. 2005, *MNRAS*, 362, 41, doi: [10.1111/j.1365-2966.2005.09321.x](https://doi.org/10.1111/j.1365-2966.2005.09321.x)
- Gardner, J. P., Mather, J. C., Abbott, R., et al. 2023, *PASP*, 135, 068001, doi: [10.1088/1538-3873/acd1b5](https://doi.org/10.1088/1538-3873/acd1b5)
- Gaskell, C. M., Goosmann, R. W., Antonucci, R. R. J., & Whysong, D. H. 2004, *ApJ*, 616, 147, doi: [10.1086/423885](https://doi.org/10.1086/423885)
- Glikman, E., Urrutia, T., Lacy, M., et al. 2012, *ApJ*, 757, 51, doi: [10.1088/0004-637X/757/1/51](https://doi.org/10.1088/0004-637X/757/1/51)
- Golubchik, M., Steinhardt, C. L., Zitrin, A., et al. 2024, arXiv e-prints, arXiv:2408.00073, doi: [10.48550/arXiv.2408.00073](https://doi.org/10.48550/arXiv.2408.00073)
- Gordon, K. D., Clayton, G. C., Misselt, K. A., Landolt, A. U., & Wolff, M. J. 2003, *ApJ*, 594, 279, doi: [10.1086/376774](https://doi.org/10.1086/376774)
- Götberg, Y., de Mink, S. E., McQuinn, M., et al. 2020, *A&A*, 634, A134, doi: [10.1051/0004-6361/201936669](https://doi.org/10.1051/0004-6361/201936669)
- Goulding, A. D., Greene, J. E., Setton, D. J., et al. 2023, *ApJL*, 955, L24, doi: [10.3847/2041-8213/acf7c5](https://doi.org/10.3847/2041-8213/acf7c5)
- Greene, J. E., Strader, J., & Ho, L. C. 2020, *ARA&A*, 58, 257, doi: [10.1146/annurev-astro-032620-021835](https://doi.org/10.1146/annurev-astro-032620-021835)
- Greene, J. E., Labbe, I., Goulding, A. D., et al. 2024, *ApJ*, 964, 39, doi: [10.3847/1538-4357/ad1e5f](https://doi.org/10.3847/1538-4357/ad1e5f)
- Hall, P. B., Anderson, S. F., Strauss, M. A., et al. 2002, *ApJS*, 141, 267, doi: [10.1086/340546](https://doi.org/10.1086/340546)
- Harikane, Y., Ouchi, M., Oguri, M., et al. 2023, *ApJS*, 265, 5, doi: [10.3847/1538-4365/acaaa9](https://doi.org/10.3847/1538-4365/acaaa9)
- Hopkins, P. F., Strauss, M. A., Hall, P. B., et al. 2004, *AJ*, 128, 1112, doi: [10.1086/423291](https://doi.org/10.1086/423291)
- Horne, K. 1986, *PASP*, 98, 609, doi: [10.1086/131801](https://doi.org/10.1086/131801)
- Inayoshi, K., & Ichikawa, K. 2024, arXiv e-prints, arXiv:2402.14706, doi: [10.48550/arXiv.2402.14706](https://doi.org/10.48550/arXiv.2402.14706)



- Inayoshi, K., & Maiolino, R. 2024, arXiv e-prints, arXiv:2409.07805. <https://arxiv.org/abs/2409.07805>
- Jakobsen, P., Ferruit, P., Alves de Oliveira, C., et al. 2022, *A&A*, 661, A80, doi: [10.1051/0004-6361/202142663](https://doi.org/10.1051/0004-6361/202142663)
- Jiang, P., Zhou, H., Ji, T., et al. 2013, *AJ*, 145, 157, doi: [10.1088/0004-6256/145/6/157](https://doi.org/10.1088/0004-6256/145/6/157)
- Jiang, Y.-F., Stone, J. M., & Davis, S. W. 2019, *ApJ*, 880, 67, doi: [10.3847/1538-4357/ab29ff](https://doi.org/10.3847/1538-4357/ab29ff)
- Jones, A. P., Tielens, A. G. G. M., Hollenbach, D. J., & McKee, C. F. 1994, *ApJ*, 433, 797, doi: [10.1086/174689](https://doi.org/10.1086/174689)
- Juodžbalis, I., Ji, X., Maiolino, R., et al. 2024, arXiv e-prints, arXiv:2407.08643, doi: [10.48550/arXiv.2407.08643](https://doi.org/10.48550/arXiv.2407.08643)
- Katz, H., Cameron, A. J., Saxena, A., et al. 2024, arXiv e-prints, arXiv:2408.03189, doi: [10.48550/arXiv.2408.03189](https://doi.org/10.48550/arXiv.2408.03189)
- Killi, M., Watson, D., Brammer, G., et al. 2023, arXiv e-prints, arXiv:2312.03065, doi: [10.48550/arXiv.2312.03065](https://doi.org/10.48550/arXiv.2312.03065)
- King, A. 2024, *MNRAS*, 531, 550, doi: [10.1093/mnras/stae1171](https://doi.org/10.1093/mnras/stae1171)
- Kocevski, D. D., Onoue, M., Inayoshi, K., et al. 2023, *ApJL*, 954, L4, doi: [10.3847/2041-8213/ace5a0](https://doi.org/10.3847/2041-8213/ace5a0)
- Kocevski, D. D., Finkelstein, S. L., Barro, G., et al. 2024, arXiv e-prints, arXiv:2404.03576, doi: [10.48550/arXiv.2404.03576](https://doi.org/10.48550/arXiv.2404.03576)
- Kokorev, V., Fujimoto, S., Labbe, I., et al. 2023, *ApJL*, 957, L7, doi: [10.3847/2041-8213/ad037a](https://doi.org/10.3847/2041-8213/ad037a)
- Kokorev, V., Caputi, K. I., Greene, J. E., et al. 2024a, *ApJ*, 968, 38, doi: [10.3847/1538-4357/ad4265](https://doi.org/10.3847/1538-4357/ad4265)
- Kokorev, V., Chisholm, J., Endsley, R., et al. 2024b, arXiv e-prints, arXiv:2407.20320, doi: [10.48550/arXiv.2407.20320](https://doi.org/10.48550/arXiv.2407.20320)
- Kokubo, M., & Harikane, Y. 2024, arXiv e-prints, arXiv:2407.04777, doi: [10.48550/arXiv.2407.04777](https://doi.org/10.48550/arXiv.2407.04777)
- Kriek, M., van Dokkum, P. G., Franx, M., et al. 2008, *ApJ*, 677, 219, doi: [10.1086/528945](https://doi.org/10.1086/528945)
- Kubota, A., & Done, C. 2019, *MNRAS*, 489, 524, doi: [10.1093/mnras/stz2140](https://doi.org/10.1093/mnras/stz2140)
- Labbe, I., Greene, J. E., Bezanson, R., et al. 2023, arXiv e-prints, arXiv:2306.07320, doi: [10.48550/arXiv.2306.07320](https://doi.org/10.48550/arXiv.2306.07320)
- Lambrides, E., Garofali, K., Larson, R., et al. 2024, arXiv e-prints, arXiv:2409.13047, doi: [10.48550/arXiv.2409.13047](https://doi.org/10.48550/arXiv.2409.13047)
- Laor, A., & Davis, S. W. 2011, *MNRAS*, 417, 681, doi: [10.1111/j.1365-2966.2011.19310.x](https://doi.org/10.1111/j.1365-2966.2011.19310.x)
- Larson, R. L., Finkelstein, S. L., Kocevski, D. D., et al. 2023, *ApJL*, 953, L29, doi: [10.3847/2041-8213/ace619](https://doi.org/10.3847/2041-8213/ace619)
- Lauer, T. R., Tremaine, S., Richstone, D., & Faber, S. M. 2007, *ApJ*, 670, 249, doi: [10.1086/522083](https://doi.org/10.1086/522083)
- Li, J., Silverman, J. D., Shen, Y., et al. 2024a, arXiv e-prints, arXiv:2403.00074, doi: [10.48550/arXiv.2403.00074](https://doi.org/10.48550/arXiv.2403.00074)
- Li, Z., Inayoshi, K., Chen, K., Ichikawa, K., & Ho, L. C. 2024b, arXiv e-prints, arXiv:2407.10760, doi: [10.48550/arXiv.2407.10760](https://doi.org/10.48550/arXiv.2407.10760)
- Lin, X., Wang, F., Fan, X., et al. 2024, arXiv e-prints, arXiv:2407.17570, doi: [10.48550/arXiv.2407.17570](https://doi.org/10.48550/arXiv.2407.17570)
- Lotz, J. M., Koekemoer, A., Coe, D., et al. 2017, *ApJ*, 837, 97, doi: [10.3847/1538-4357/837/1/97](https://doi.org/10.3847/1538-4357/837/1/97)
- Lupi, A., Trinca, A., Volonteri, M., Dotti, M., & Mazzucchelli, C. 2024, arXiv e-prints, arXiv:2406.17847, doi: [10.48550/arXiv.2406.17847](https://doi.org/10.48550/arXiv.2406.17847)
- Ma, Y., Goulding, A., Greene, J. E., et al. 2024, arXiv e-prints, arXiv:2401.04177, doi: [10.48550/arXiv.2401.04177](https://doi.org/10.48550/arXiv.2401.04177)
- Maiolino, R., Marconi, A., Salvati, M., et al. 2001, *A&A*, 365, 28, doi: [10.1051/0004-6361:20000177](https://doi.org/10.1051/0004-6361:20000177)
- Maiolino, R., Scholtz, J., Curtis-Lake, E., et al. 2023, arXiv e-prints, arXiv:2308.01230, doi: [10.48550/arXiv.2308.01230](https://doi.org/10.48550/arXiv.2308.01230)
- Maiolino, R., Risaliti, G., Signorini, M., et al. 2024a, arXiv e-prints, arXiv:2405.00504, doi: [10.48550/arXiv.2405.00504](https://doi.org/10.48550/arXiv.2405.00504)
- Maiolino, R., Scholtz, J., Witstok, J., et al. 2024b, *Nature*, 627, 59, doi: [10.1038/s41586-024-07052-5](https://doi.org/10.1038/s41586-024-07052-5)
- Matthee, J., Naidu, R. P., Brammer, G., et al. 2024, *ApJ*, 963, 129, doi: [10.3847/1538-4357/ad2345](https://doi.org/10.3847/1538-4357/ad2345)
- Naab, T., Johansson, P. H., & Ostriker, J. P. 2009, *ApJL*, 699, L178, doi: [10.1088/0004-637X/699/2/L178](https://doi.org/10.1088/0004-637X/699/2/L178)
- Narayanan, D., Conroy, C., Davé, R., Johnson, B. D., & Popping, G. 2018, *ApJ*, 869, 70, doi: [10.3847/1538-4357/aaed25](https://doi.org/10.3847/1538-4357/aaed25)
- Newman, A. B., Treu, T., Ellis, R. S., et al. 2013, *ApJ*, 765, 24, doi: [10.1088/0004-637X/765/1/24](https://doi.org/10.1088/0004-637X/765/1/24)
- Noll, S., Pierini, D., Cimatti, A., et al. 2009, *A&A*, 499, 69, doi: [10.1051/0004-6361/200811526](https://doi.org/10.1051/0004-6361/200811526)
- Osterbrock, D. E., & Ferland, G. J. 2006, *Astrophysics of gaseous nebulae and active galactic nuclei*
- Pacucci, F., & Narayan, R. 2024, arXiv e-prints, arXiv:2407.15915, doi: [10.48550/arXiv.2407.15915](https://doi.org/10.48550/arXiv.2407.15915)
- Pacucci, F., Nguyen, B., Carniani, S., Maiolino, R., & Fan, X. 2023, *ApJL*, 957, L3, doi: [10.3847/2041-8213/ad0158](https://doi.org/10.3847/2041-8213/ad0158)
- Pérez-González, P. G., Barro, G., Rieke, G. H., et al. 2024, *ApJ*, 968, 4, doi: [10.3847/1538-4357/ad38bb](https://doi.org/10.3847/1538-4357/ad38bb)
- Price, S. H., Bezanson, R., Labbe, I., et al. 2024, arXiv e-prints, arXiv:2408.03920, doi: [10.48550/arXiv.2408.03920](https://doi.org/10.48550/arXiv.2408.03920)



- Reinoso, B., Klessen, R. S., Schleicher, D., Glover, S. C. O., & Solar, P. 2023, *MNRAS*, 521, 3553, doi: [10.1093/mnras/stad790](https://doi.org/10.1093/mnras/stad790)
- Salim, S., & Narayanan, D. 2020, *ARA&A*, 58, 529, doi: [10.1146/annurev-astro-032620-021933](https://doi.org/10.1146/annurev-astro-032620-021933)
- Sánchez-Blázquez, P., Peletier, R. F., Jiménez-Vicente, J., et al. 2006, *MNRAS*, 371, 703, doi: [10.1111/j.1365-2966.2006.10699.x](https://doi.org/10.1111/j.1365-2966.2006.10699.x)
- Schaerer, D., Guibert, J., Marques-Chaves, R., & Martins, F. 2024, arXiv e-prints, arXiv:2407.12122, doi: [10.48550/arXiv.2407.12122](https://doi.org/10.48550/arXiv.2407.12122)
- Sesar, B., Ivezić, Ž., Lupton, R. H., et al. 2007, *AJ*, 134, 2236, doi: [10.1086/521819](https://doi.org/10.1086/521819)
- Shakura, N. I., & Sunyaev, R. A. 1973, *A&A*, 24, 337
- Stasińska, G., & Izotov, Y. 2001, *A&A*, 378, 817, doi: [10.1051/0004-6361:20011303](https://doi.org/10.1051/0004-6361:20011303)
- Suess, K. A., Williams, C. C., Robertson, B., et al. 2023, *ApJL*, 956, L42, doi: [10.3847/2041-8213/acf5e6](https://doi.org/10.3847/2041-8213/acf5e6)
- Suess, K. A., Weaver, J. R., Price, S. H., et al. 2024, arXiv e-prints, arXiv:2404.13132, doi: [10.48550/arXiv.2404.13132](https://doi.org/10.48550/arXiv.2404.13132)
- Sun, W., Ho, L. C., Zhuang, M.-Y., et al. 2024, *ApJ*, 960, 104, doi: [10.3847/1538-4357/acflf6](https://doi.org/10.3847/1538-4357/acflf6)
- Szomoru, D., Franx, M., & van Dokkum, P. G. 2012, *ApJ*, 749, 121, doi: [10.1088/0004-637X/749/2/121](https://doi.org/10.1088/0004-637X/749/2/121)
- Temple, M. J., Hewett, P. C., & Banerji, M. 2021, *MNRAS*, 508, 737, doi: [10.1093/mnras/stab2586](https://doi.org/10.1093/mnras/stab2586)
- Thomas, A. D., Groves, B. A., Sutherland, R. S., et al. 2016, *ApJ*, 833, 266, doi: [10.3847/1538-4357/833/2/266](https://doi.org/10.3847/1538-4357/833/2/266)
- Thompson, T. A., Quataert, E., & Murray, N. 2005, *ApJ*, 630, 167, doi: [10.1086/431923](https://doi.org/10.1086/431923)
- Trayford, J. W., Lagos, C. d. P., Robotham, A. S. G., & Obreschkow, D. 2020, *MNRAS*, 491, 3937, doi: [10.1093/mnras/stz3234](https://doi.org/10.1093/mnras/stz3234)
- van Dokkum, P., & Conroy, C. 2024, *ApJL*, 973, L32, doi: [10.3847/2041-8213/ad77b8](https://doi.org/10.3847/2041-8213/ad77b8)
- van Dokkum, P. G., Franx, M., Kriek, M., et al. 2008, *ApJL*, 677, L5, doi: [10.1086/587874](https://doi.org/10.1086/587874)
- van Dokkum, P. G., Whitaker, K. E., Brammer, G., et al. 2010, *ApJ*, 709, 1018, doi: [10.1088/0004-637X/709/2/1018](https://doi.org/10.1088/0004-637X/709/2/1018)
- Vanzella, E., Claeysens, A., Welch, B., et al. 2023, *ApJ*, 945, 53, doi: [10.3847/1538-4357/acb59a](https://doi.org/10.3847/1538-4357/acb59a)
- Voggel, K. T., Seth, A. C., Baumgardt, H., et al. 2019, *ApJ*, 871, 159, doi: [10.3847/1538-4357/aaf735](https://doi.org/10.3847/1538-4357/aaf735)
- Volonteri, M., Haardt, F., & Gültekin, K. 2008, *MNRAS*, 384, 1387, doi: [10.1111/j.1365-2966.2008.12911.x](https://doi.org/10.1111/j.1365-2966.2008.12911.x)
- Volonteri, M., Reines, A. E., Atek, H., Stark, D. P., & Trebitsch, M. 2017, *ApJ*, 849, 155, doi: [10.3847/1538-4357/aa93f1](https://doi.org/10.3847/1538-4357/aa93f1)
- Wang, B., de Graaff, A., Davies, R. L., et al. 2024a, arXiv e-prints, arXiv:2403.02304, <https://arxiv.org/abs/2403.02304>
- Wang, B., Leja, J., de Graaff, A., et al. 2024b, *ApJL*, 969, L13, doi: [10.3847/2041-8213/ad55f7](https://doi.org/10.3847/2041-8213/ad55f7)
- Weaver, J. R., Cutler, S. E., Pan, R., et al. 2024, *ApJS*, 270, 7, doi: [10.3847/1538-4365/ad07e0](https://doi.org/10.3847/1538-4365/ad07e0)
- Weibel, A., de Graaff, A., Setton, D. J., et al. 2024, arXiv e-prints, arXiv:2409.03829, doi: [10.48550/arXiv.2409.03829](https://doi.org/10.48550/arXiv.2409.03829)
- Williams, C. C., Alberts, S., Ji, Z., et al. 2024, *ApJ*, 968, 34, doi: [10.3847/1538-4357/ad3f17](https://doi.org/10.3847/1538-4357/ad3f17)
- Wright, L., Whitaker, K. E., Weaver, J. R., et al. 2024, *ApJL*, 964, L10, doi: [10.3847/2041-8213/ad2b6d](https://doi.org/10.3847/2041-8213/ad2b6d)
- Yue, M., Eilers, A.-C., Ananna, T. T., et al. 2024, arXiv e-prints, arXiv:2404.13290, doi: [10.48550/arXiv.2404.13290](https://doi.org/10.48550/arXiv.2404.13290)
- Zakamska, N. L., Schmidt, G. D., Smith, P. S., et al. 2005, *AJ*, 129, 1212, doi: [10.1086/427543](https://doi.org/10.1086/427543)
- Zakamska, N. L., Strauss, M. A., Krolik, J. H., et al. 2006, *AJ*, 132, 1496, doi: [10.1086/506986](https://doi.org/10.1086/506986)
- Zitrin, A., Fabris, A., Merten, J., et al. 2015, *ApJ*, 801, 44, doi: [10.1088/0004-637X/801/1/44](https://doi.org/10.1088/0004-637X/801/1/44)